

# Many-body quadrupolar sum rule for higher-order topological insulators

Wonjun Lee,<sup>1,2,\*</sup> Gil Young Cho,<sup>1,2,3,†</sup> and Byungmin Kang<sup>4,‡</sup>

<sup>1</sup>*Department of Physics, Pohang University of Science and Technology, Pohang 37673, Republic of Korea*

<sup>2</sup>*Center for Artificial Low Dimensional Electronic Systems, Institute for Basic Science, Pohang 37673, Republic of Korea*

<sup>3</sup>*Asia Pacific Center for Theoretical Physics, Pohang 37673, Republic of Korea*

<sup>4</sup>*School of Physics, Korea Institute for Advanced Study, Seoul 02455, Korea*



(Received 7 November 2021; revised 13 January 2022; accepted 6 April 2022; published 21 April 2022)

The modern theory of polarization establishes the bulk-boundary correspondence for the bulk polarization. In this paper, we attempt to extend it to a sum rule of the bulk quadrupole moment by employing a many-body operator introduced in Kang *et al.* [B. Kang, K. Shiozaki, and G. Y. Cho, *Phys. Rev. B* **100**, 245134 (2019)] and Wheeler *et al.* [W. A. Wheeler, L. K. Wagner, and T. L. Hughes, *Phys. Rev. B* **100**, 245135 (2019)]. The sum rule that we propose consists of the alternating sum of four observables, which are the phase factors of the many-body operator in different boundary conditions. We demonstrate its validity through extensive numerical computations for various noninteracting tight-binding models. We also observe that individual terms in the sum rule correspond to the bulk quadrupole moment, the edge-localized polarizations, and the corner charge in the thermodynamic limit on some models.

DOI: [10.1103/PhysRevB.105.155143](https://doi.org/10.1103/PhysRevB.105.155143)

## I. INTRODUCTION

Recent developments in topological insulators [1,2] uncovered a new class of topological material, called higher-order topological insulators (HOTIs) [3–5]. It was found that HOTIs are not just conceptual ideas as there are material proposals [6,7] as well as material realizations [8,9] of them. HOTIs are characterized by nontrivial boundary-of-boundary states despite that the boundaries are trivial. Among various theoretical tools, the bulk polarization has proven useful in understanding many aspects of topological insulators [10–14]. It is therefore natural to ask if the bulk quadrupole or higher multipole moments could play the same role for HOTIs.

The modern theory of polarization [15–17] identifies the bulk polarization with the sum of Wannier centers. Later, the bulk polarization of a many-body state is shown to be identified as the phase factor of the expectation value of a many-body operator [18]. Despite the success of the modern theory of polarization, the modern theory of quadrupole and higher multipole moments has not been fully developed so far. One attempt is to employ the Wannier centers to define the bulk quadrupole moment, but this approach has been successful when there exist crystalline symmetries so that the bulk multipole moment is quantized [4,19]. On the other line of development, Refs. [20,21] introduced a many-body operator  $\hat{U}_2$  for the quadrupole moment generalizing the many-body operator presented in Ref. [18]:

$$\hat{U}_2 \equiv \exp \left[ \frac{2\pi i}{L_x L_y} \sum_{x,y=1}^{L_x, L_y} xy (\hat{n}_{x,y} - n_e) \right],$$

where  $\hat{n}_{x,y}$  is the number operator, and  $n_e$  is the background charge. This approach can in principle be applied to systems without any crystalline symmetries and to interacting systems; however, the observables given by  $\hat{U}_2$  have difficulties in identifying their physical meanings with respect to their coordinate dependence [20] and lack of periodicity [22] so their physical meanings have not been fully understood yet.

One of the successes of the modern theory of polarization is that it identifies the bulk polarization with the boundary charge, which is called the bulk-boundary correspondence [17,23]. While the bulk polarization is determined by a full many-body electron state, the boundary charge is determined by a simple one-body observable near the boundary. Thus, the identification of the two is rather surprising and also provides a firm justification of the modern theory of polarization. A natural question is then whether such a correspondence for HOTIs can be formulated in terms of the bulk quadrupole moment. In recent studies, the bulk-boundary correspondences for HOTIs were formulated in terms of the filling anomaly with rotation symmetries [24–28], in terms of the bulk quadrupole moment with inversion symmetry [29,30], and in terms of the adiabatic current flowing along the edges [31]. The bulk-boundary correspondences in terms of the quadrupole moment were presented using Wannier functions, where the corner charge is expressed as a sum of quantities that depend on the choice of the bulk Wannier functions, although the corner charge itself is not.

In this paper, we propose another bulk-boundary correspondence in terms of the operator  $\hat{U}_2$ , which is given by an alternating sum of four phase factors, where the sum vanishes in the thermodynamic limit:

$$\phi_{pp} - \phi_{op} - \phi_{po} + \phi_{oo} = 0 \pmod{1}.$$

Four phase factors are the phase factors of the expectation values of  $\hat{U}_2$  with respect to the ground state in different

\* wonjun1998@postech.ac.kr

† gilyoungcho@postech.ac.kr

‡ bkang119@kias.re.kr

boundary conditions:

$$\phi_{ab} = \frac{1}{2\pi} \text{Im}\{\log[\langle \text{GS}(a, b) | \hat{U}_2 | \text{GS}(a, b) \rangle]\},$$

where  $a$  and  $b$  refer to the boundary conditions along the  $x$  and  $y$  direction, respectively, with  $a$  and  $b$  being either  $p$  (periodic) or  $o$  (open). We observe that for band insulators having well-localized edge-localized polarizations defined in Ref. [4] based on the hybrid Wannier function (HWF), the phase factors  $\phi_{pp}$ ,  $\phi_{po/op}$ , and  $\phi_{oo}$  can be identified with the bulk quadrupole moment, the edge-localized polarizations, and the corner charge, respectively, which consequently elevates our bulk-boundary correspondence to that for the quadrupole moment. We further observe that for some insulators, there exist HWFs with the corresponding hybrid Wannier value at 0.5 so that one cannot directly apply the definition of the edge-localized polarization presented in Ref. [4] due to its branch cut dependence, as elaborated in Appendix F. For those insulators, we find that at least the phase factor  $\phi_{oo}$  can be regarded as the corner charge in the thermodynamic limit while the physical meaning of the other phase factors becomes unclear.

The paper is organized as follows. In Sec. II, we introduce sum rules encoding the bulk-boundary correspondence for multipole moments using many-body operators. In Sec. III, we provide numerical results presenting our observations in Sec. II. We conclude in Sec. IV where the summary of main results is given and possible future directions are discussed. In Appendix A, we derive the dipolar and quadrupolar sum rules for classical systems. In Appendix B, we give field theoretic justifications of the interpretations of the phase factors  $\phi_{ab}$ . In Appendix C, we provide a proof that the many-body operator can measure the corner charge in one-dimensional (1D) geometry for band insulators. In Appendix D, we discuss the coordinate dependence of the phase factor  $\phi_{op}$ . In Appendix E, we provide numerical results for a  $C_3$ -symmetric insulator, which suggests that the sum rule may hold in other types of symmetric insulators besides the  $C_4$ -symmetric ones discussed in the main text. Finally, in Appendix F, we provide technical remarks on the HWF-based edge-localized polarization including the branch cut dependence which becomes more explicit for the models with the hybrid Wannier value at 0.5.

## II. MULTIPOLAR SUM RULES

In the following, we present the multipolar sum rules for quantum systems in one and two dimensions. For concreteness, we make here some remarks on the sum rules. First, we only focus on one-dimensional systems having nonzero bulk polarization in Sec. II A and two-dimensional (2D) systems with vanishing bulk polarization in Sec. II B. Second, we focus on circle/line geometry for one-dimensional systems and torus/cylinder/rectangle geometry for two-dimensional systems. Each geometry is characterized by open or periodic boundary conditions. In addition, we always use hard-cutoff boundary conditions for open boundaries. Third, for simplicity we restrict the position of each orbital at a Bravais lattice site. Fourth, for all the quantum systems presented below, we assume translation symmetry and  $C_2$  symmetry, which includes the cases where the corner charge is not quantized.

Finally, for convenience, we set the electron charge to 1 in the following discussions.

### A. Dipolar sum rule

In this subsection, we introduce the dipolar sum rule for many-body quantum systems as a generalization of the classical dipolar sum rule. The dipolar sum rule relates the bulk polarization with the boundary charge. To motivate the quantum mechanical dipolar sum rule, we first state the classical dipolar sum rule:

$$Q_c = \mathcal{P}, \quad (1)$$

where  $\mathcal{P}$  and  $Q_c$  are the classical bulk polarization and boundary charge, respectively. The derivation of Eq. (1) and the definitions of the electric moments can be found in Appendix A 1.

We now generalize the classical dipolar sum rule Eq. (1) to a one-dimensional quantum mechanical system. To this end, we first need to define the bulk polarization and the boundary charge for a quantum system. The boundary charge can be defined as a one-body observable:

$$Q_c^{(1)} \equiv \sum_{x=1}^{L_x/2} [\rho(x) - n_e] \pmod{1}, \quad (2)$$

where  $L_x$  is the total system size,  $\rho(x) = \langle \hat{n}_x \rangle = \langle \sum_{\alpha=1}^{N_{\text{orb}}} c_{x,\alpha}^\dagger c_{x,\alpha} \rangle$  is the charge density at site  $x$  with the number of orbitals per site  $N_{\text{orb}}$ , and  $n_e$  is the average number of electrons per site. We then employ Resta's many-body operator [18]:

$$\hat{U}_1 \equiv \exp \left[ \frac{2\pi i}{L_x} \sum_{x=1}^{L_x} x(\hat{n}_x - n_e) \right], \quad (3)$$

where we include the background charge  $n_e$  from ions sitting at each lattice site. Using  $\hat{U}_1$ , the bulk polarization is given by

$$P = \frac{1}{2\pi} \text{Im}\{\log(\langle \text{GS} | \hat{U}_1 | \text{GS} \rangle)\}, \quad (4)$$

where  $|\text{GS}\rangle$  is the many-body ground state subject to the periodic boundary condition. With these, the classical dipolar sum rule Eq. (1) generalizes as [17,23]

$$Q_c^{(1)} = P \pmod{1} \quad (5)$$

in quantum systems. Unlike the dipole sum rule in classical systems, Eq. (5) holds only modulo 1, the unit of electron charge.

Having obtained the sum rule for the dipole moment, we consider the further characterization solely in terms of the many-body operator  $\hat{U}_1$ . For this, we define the phase factor  $\phi_a$  of the expectation value of  $\hat{U}_1$  as

$$\phi_a \equiv \frac{1}{2\pi} \text{Im}\{\log[\langle \text{GS}(a) | \hat{U}_1 | \text{GS}(a) \rangle]\}, \quad (6)$$

where  $|\text{GS}(a)\rangle$  is the ground state under the boundary conditions of type  $a$  which can be either  $p$  (periodic) or  $o$  (open).

While it seems not widely known, the boundary charge can also be captured from  $\phi_o$  in the thermodynamic limit, i.e.,

$$Q_c^{(1)} = \phi_o \pmod{1} \quad (7)$$

as the system size goes to infinity when the system is gapped. Our proof of Eq. (7) for band insulators can be found in Appendix C. Thus, by combining Eqs. (4) and (7), the dipole sum rule can be succinctly recast in terms of the phase factors:

$$\phi_p = \phi_o \pmod{1}. \quad (8)$$

### B. Quadrupolar sum rule

In this subsection, we introduce the quadrupolar sum rule for many-body quantum systems, which generalizes the quantum mechanical dipolar sum rule to the quadrupole case, and discuss its difficulties for certain cases in identifying the physical meaning of individual terms in the sum rule.

The quadrupole sum rule would relate the bulk quadrupole moment, the edge-localized polarization, and the corner charge [4,20] if these quantities are well defined. To illustrate the quadrupolar sum rule, we first need to state the classical quadrupolar sum rule:

$$Q_c = -Q_{xy} + \mathcal{P}_x^{\text{edge}} + \mathcal{P}_y^{\text{edge}}, \quad (9)$$

where  $Q_{xy}$ ,  $\mathcal{P}_{x/y}^{\text{edge}}$ , and  $Q_c$  are the classical bulk-quadrupole moment, the edge-localized polarizations, and the corner charge, respectively. The derivation of Eq. (9) and the definitions of the classical electric moments can be found in Appendix A 2.

A natural generalization of the classical quadrupolar sum rule to the quantum mechanical one in two dimensions would be

$$Q_c^{(2)} = -Q_{xy} + P_x^{\text{edge}} + P_y^{\text{edge}} \pmod{1}, \quad (10)$$

where  $Q_c^{(2)}$  is the corner charge of a two-dimensional system of the size  $L_x \times L_y$ :

$$Q_c^{(2)} \equiv \sum_{x=1}^{L_x/2} \sum_{y=1}^{L_y/2} (\rho(x, y) - n_e) \pmod{1}, \quad (11)$$

with  $\rho(x, y) = \langle \hat{n}_{x,y} \rangle = \langle \sum_{\alpha=1}^{N_{\text{orb}}} c_{x,y,\alpha}^\dagger c_{x,y,\alpha} \rangle$  being the local charge density, and where  $Q_{xy}$  and  $P_{x/y}^{\text{edge}}$  are the quantum mechanical bulk quadrupole moment and the edge-localized polarizations, respectively. As a side note, our corner charge [Eq. (11)] corresponds to the bare corner charge in Ref. [30]. We remark that the edge-localized polarizations  $P_{x/y}^{\text{edge}}$  include the contribution from a dressing of polarized one-dimensional chains along the boundaries [32], which does not affect the quadrupolar sum rule Eq. (10), and are fixed for a given state. The precise forms of  $Q_{xy}$  and  $P_{x/y}^{\text{edge}}$  will be presented below.

Similar to the dipole case, let us introduce the following many-body operator [20,21]:

$$\hat{U}_2 \equiv \exp \left[ \frac{2\pi i}{L_x L_y} \sum_{x,y=1}^{L_x, L_y} xy (\hat{n}_{x,y} - n_e) \right], \quad (12)$$

where  $\hat{n}_{x,y}$  is the electron number operator at  $(x, y)$  and  $L_x$  ( $L_y$ ) is the linear system size in the  $x$  direction ( $y$  direction). For the open boundary, we assign the coordinate  $x = 1$  ( $y = 1$ ) to sites on the left (bottom) boundary and the coordinate  $x = L_x$  ( $y = L_y$ ) to sites on the right (top) boundary. For the periodic boundary, the  $x$  coordinate ( $y$  coordinate) could be assigned

arbitrary as long as it starts from 1 and ends with  $L_x$  ( $L_y$ ) since it does not change the expectation value of  $\hat{U}_2$  with respect to a translation invariant state.

In order to formulate the quadrupolar sum rule in terms of the phase factors of the expectation values of  $\hat{U}_2$ , we first introduce

$$\phi_{ab} = \frac{1}{2\pi} \text{Im} \{ \log [ \langle \text{GS}(a, b) | \hat{U}_2 | \text{GS}(a, b) \rangle ] \}, \quad (13)$$

where  $|\text{GS}(a, b)\rangle$  is the ground state under the  $a$  and  $b$  boundary conditions along the  $x$  and  $y$  direction, respectively, with  $a$  and  $b$  being either  $p$  (periodic) or  $o$  (open). Each boundary condition corresponds to different geometry; for example,  $pp$  and  $po$  mean the torus and the cylinder geometry, respectively. As a note, the phase factor  $\phi_{op}$  ( $\phi_{po}$ ) is guaranteed to be invariant under the coordinate transformation  $y \rightarrow y + L_y$  ( $x \rightarrow x + L_x$ ) in the thermodynamic limit if the system has translation symmetry along the  $y(x)$  direction, and if the limit of  $L_x(L_y) \rightarrow \infty$  is taken first. Even though the invariance of  $\phi_{op}$  is not guaranteed on the 2D limit  $L_x = L_y = L \rightarrow \infty$ , the thermodynamic values of  $\phi_{ab}$  presented in Tables I–VI are extrapolated on the 2D limit as we empirically check that the convergence values do not depend on the order of limits. Details regarding the coordinate dependence of  $\phi_{op/po}$  are discussed in Appendix D.

Using these phase factors, we propose the bulk-boundary correspondence in terms of the phase factors as

$$\phi_{pp} - \phi_{op} - \phi_{po} + \phi_{oo} = 0 \pmod{1} \quad (14)$$

and numerically find that this holds in the thermodynamic limit on band insulators. We will call this the sum rule of the phase factors, or simply the sum rule. In addition, we also find that  $\phi_{oo}$  agrees with  $Q_c^{(2)}$ :

$$Q_c^{(2)} = \phi_{oo} \pmod{1}. \quad (15)$$

As a demonstration, we provide numerical confirmations of these on band insulators in Sec. III. The above two equations, i.e., Eqs. (14) and (15), are the main results of our present paper.

Based on the identification of the corner charge [Eq. (15)] and the comparison between two sum rules, Eqs. (10) and (14) suggest that  $\phi_{pp}$  can be naturally identified with the bulk quadrupole moment:

$$Q_{xy} = \phi_{pp} \pmod{1}, \quad (16)$$

which has been checked for the cases with nontrivial bulk quadrupole moment [20,21]. In addition,  $\phi_{po/op}$  are identified with the edge-localized polarizations:

$$P_x^{\text{edge}} = \phi_{po} \pmod{1}, \quad P_y^{\text{edge}} = \phi_{op} \pmod{1}. \quad (17)$$

The above identifications of the phase factors  $\phi_{ab}$  can also be justified using the effective field theoretic description of multipole moments which is summarized in Appendix B. Whenever these identifications can be made, the sum rule Eq. (14) indeed becomes the quadrupole sum rule for quantum systems. In Sec. III A, we numerically demonstrate the validity of the identifications of  $\phi_{po/op}$  by comparing these with the HWF-based edge-localized polarizations defined in Ref. [4]. However, it is important to note that these identifications are not always possible. In Sec. III B, we provide an example in

TABLE I. The phase factors  $\phi_{ab}$  in Eq. (13) and the electric moments ( $Q_c^{(2)}$ ,  $\tilde{P}_x^{\text{edge}}$ ,  $\tilde{P}_y^{\text{edge}}$ ) in Eqs. (11) and (18) are computed for the quadrupole insulator [Eq. (20)] with various parameters. The sum of the phase factors  $\sum(-1)^{ab}\phi_{ab}$  in the last column refers to the combination  $\phi_{pp} - \phi_{po} - \phi_{op} + \phi_{oo}$  as per Eq. (14). All values are the ones from extrapolating the observables as a function of  $1/L$ , where we consider isotropic systems  $L_x = L_y = L$  with  $L$  from 23 to 30. An explicit extrapolation procedure is presented in Fig. 1. We use round brackets to denote the errors of the least significant digit. We see that the edge-localized polarizations  $\tilde{P}_x^{\text{edge}}$  and  $\tilde{P}_y^{\text{edge}}$  agree with phase factors  $\phi_{po}$  and  $\phi_{op}$ , corner charge  $Q_c^{(2)}$  agrees with  $\phi_{oo}$ , and the sum rule is satisfied up to small errors.

Model parameters	Phase factors				Electric moments			Sum rule
	$\phi_{pp}$	$\phi_{po}$	$\phi_{op}$	$\phi_{oo}$	$Q_c^{(2)}$	$\tilde{P}_x^{\text{edge}}$	$\tilde{P}_y^{\text{edge}}$	$\sum(-1)^{ab}\phi_{ab}$
$H_{\text{quad}}(\gamma_x, \gamma_y, \lambda_x, \lambda_y, \delta)$								
(0.1, 0.1, 1.0, 1.0, $10^{-7}$ )	0.50000(0)	0.50000(0)	0.50000(0)	0.50000(0)	0.50000(0)	0.50000(0)	0.50000(0)	0.00000(0)
(0.5, 0.5, 1.0, 1.0, 0.7)	-0.11389(0)	-0.11385(0)	-0.11385(0)	-0.11392(0)	-0.11387(0)	-0.11386(0)	-0.11386(0)	-0.00010(0)
(0.2, 0.3, 1.0, 1.0, 0.1)	-0.43156(0)	-0.43155(0)	-0.43155(0)	-0.43155(0)	-0.43156(0)	-0.43156(0)	-0.43155(0)	-0.00001(0)
(0.1, 0.1, 1.0, 1.2, 0.1)	-0.44018(0)	-0.44017(0)	-0.44018(0)	-0.44019(0)	-0.44018(0)	-0.44018(0)	-0.44018(0)	-0.00002(0)

which these identifications fail as  $\phi_{pp}$ ,  $\phi_{op}$ , and  $\phi_{po}$  are not convergent in the thermodynamic limit. Nonetheless, even for these cases, the sum rule Eq. (14) and the identification of the corner charge with  $\phi_{oo}$  [Eq. (15)] always hold.

In the remainder of this section, we briefly discuss the HWF-based edge-localized polarization [4]:

$$\tilde{P}_x^{\text{edge}} = \sum_j \sum_{y=1}^{L_y/2} v^j \rho^j(y) \pmod{1}, \quad (18)$$

where  $\rho^j(y)$  is the density, and  $e^{2\pi i v_j}$  is the eigenvalue of the  $j$ th HWF  $\psi^j(y)$  of the hybrid Wilson loop  $\mathcal{W}_{k_x}$  along the  $x$  direction. We find that for band insulators having well-localized  $\tilde{P}_{x/y}^{\text{edge}}$  along the boundaries,  $\tilde{P}_{x/y}^{\text{edge}}$  and  $\phi_{po/op}$  seem to agree with each other in the thermodynamic limit and the same quantized value for insulators having  $C_4$  symmetry:

$$\tilde{P}_x^{\text{edge}} = \phi_{op} \pmod{1}, \quad \tilde{P}_y^{\text{edge}} = \phi_{po} \pmod{1}. \quad (19)$$

However,  $\tilde{P}_{x/y}^{\text{edge}}$  crucially depends on the choice of the branch cut of the hybrid Wannier values. In particular, for the models with the hybrid Wannier value at 0.5, this dependence becomes more explicit, thereby leading to a difficulty in computing  $\tilde{P}_{x/y}^{\text{edge}}$ . We discuss this branch cut dependence in more detail in Appendix F.

### III. NUMERICAL DEMONSTRATION

In this section, we provide numerical demonstrations of the sum rule Eq. (14) and observations, Eqs. (15) and (19). Due

TABLE II. The phase factors  $\phi_{ab}$  and the electric moments ( $Q_c^{(2)}$ ,  $\tilde{P}_x^{\text{edge}}$ ,  $\tilde{P}_y^{\text{edge}}$ ) with are computed for the edge-localized polarization insulator [Eq. (21)] with various parameters. Here we use the same extrapolation procedure as in Table I. In this case as well, the edge-localized polarizations  $\tilde{P}_x^{\text{edge}}$  and  $\tilde{P}_y^{\text{edge}}$  agree with phase factors  $\phi_{po}$  and  $\phi_{op}$ , corner charge  $Q_c^{(2)}$  agrees with  $\phi_{oo}$ , and the sum rule is satisfied up to small errors.

Model parameters	Phase factors				Electric moments			Sum rule
	$\phi_{pp}$	$\phi_{po}$	$\phi_{op}$	$\phi_{oo}$	$Q_c^{(2)}$	$\tilde{P}_x^{\text{edge}}$	$\tilde{P}_y^{\text{edge}}$	$\sum(-1)^{ab}\phi_{ab}$
$H_{\text{edge}}(\gamma_x, \gamma_y, \lambda_x, \lambda_y, \delta)$								
(0.1, 0.1, 1, 1.2, $10^{-7}$ )	0.00000(0)	0.50000(0)	0.00000(0)	0.50000(0)	0.50000(0)	0.50000(0)	0.00000(0)	0.00000(0)
(0.5, 0.5, 1.0, 1.0, 0.7)	-0.01661(0)	-0.09914(0)	-0.09914(0)	-0.18179(0)	-0.18174(0)	-0.09836(0)	-0.09836(0)	-0.00012(0)
(0.2, 0.3, 1.0, 1.0, 0.1)	-0.05940(1)	-0.27871(1)	-0.31926(1)	0.46139(1)	0.46122(1)	-0.27833(1)	-0.31897(1)	-0.00004(1)
(0.1, 0.1, 1.0, 1.2, 0.1)	-0.01585(0)	-0.44086(0)	-0.12064(0)	0.45436(0)	0.45434(0)	-0.44172(0)	-0.11936(0)	0.00002(0)

to size limitation, our numerics are based on noninteracting tight-binding models on the square lattice. However, we believe that the same sum rule should also hold in interacting cases as well, since our formalism is based on many-body operators. In addition, we separately discuss models without and with the hybrid Wannier value at 0.5 as there exists a difficulty in computing  $\tilde{P}_{x/y}^{\text{edge}}$  for the latter case. We therefore numerically confirm the validity of Eq. (19) only for the former case while the numerical confirmations of the sum rule Eq. (14) and the identification of  $\phi_{oo}$  with  $Q_c^{(2)}$  [Eq. (15)] are presented in all cases.

#### A. Models without the hybrid Wannier value at 0.5

We present numerical results on models without the hybrid Wannier value at 0.5. Tested models are the quadrupole insulator, the edge-localized polarization insulator, the quadrupole insulator with  $\pi/2$  flux per plaquette, and the two band model introduced in Ref. [33], where details of these models can be found below. In the case of full open boundary conditions, the  $C_4$  symmetry breaking term is always introduced in order to split the possible degeneracy at the Fermi level. Due to such term, the number of filled states is always equal to the filling  $n_e/N_{\text{orb}}$  times the number of sites  $N$ . The same  $C_4$  breaking term often splits the degeneracy of the hybrid Wannier values at 0.5 in the case of mixed open and periodic boundary conditions.

For each model, we numerically compute the phase factors  $\phi_{ab}$  [Eq. (13)], the edge-localized polarizations  $\tilde{P}_{x/y}^{\text{edge}}$  [Eq. (18)], and the corner charge  $Q_c^{(2)}$  [Eq. (11)] for

TABLE III. The phase factors  $\phi_{ab}$  and the electric moments ( $Q_c^{(2)}$ ,  $\tilde{P}_x^{\text{edge}}$ ,  $\tilde{P}_y^{\text{edge}}$ ) are computed for the quadrupole insulator with  $\pi/2$  flux per plaquette [Eq. (22)] with various parameters. Here we use the same extrapolation procedure as in Table I. In this case as well, the edge-localized polarizations  $\tilde{P}_x^{\text{edge}}$  and  $\tilde{P}_y^{\text{edge}}$  agree with phase factors  $\phi_{po}$  and  $\phi_{op}$ , corner charge  $Q_c^{(2)}$  agrees with  $\phi_{oo}$ , and the sum rule is satisfied up to small errors.

Model parameters	Phase factors				Electric moments			Sum rule
$H_{\text{quad}}^{(\pi/2)}(\gamma_x, \gamma_y, \lambda_x, \lambda_y, \delta)$	$\phi_{pp}$	$\phi_{po}$	$\phi_{op}$	$\phi_{oo}$	$Q_c^{(2)}$	$\tilde{P}_x^{\text{edge}}$	$\tilde{P}_y^{\text{edge}}$	$\sum(-1)^{ab}\phi_{ab}$
(0.1, 0.1, 1.0, 1.0, $10^{-7}$ )	0.50000(0)	0.50000(0)	0.50000(0)	0.50000(0)	0.50000(0)	0.50000(0)	0.50000(0)	0.00000(0)
(0.5, 0.5, 1.0, 1.0, 0.7)	-0.06272(0)	-0.09622(0)	-0.09622(0)	-0.12980(0)	-0.12975(0)	-0.09675(0)	-0.09675(0)	-0.00009(0)
(0.2, 0.3, 1.0, 1.0, 0.1)	-0.40237(0)	-0.42169(0)	-0.42104(0)	-0.44037(0)	-0.44039(0)	-0.42192(0)	-0.42155(0)	-0.00001(0)
(0.1, 0.1, 1.0, 1.2, 0.1)	-0.42101(0)	-0.43853(0)	-0.43160(0)	-0.44913(0)	-0.44913(0)	-0.43855(0)	-0.43165(0)	-0.00001(0)

various parameters. The results are summarized in Tables I, II, and III. All observables in the tables are the extrapolated values in the thermodynamic limit  $L \rightarrow \infty$  which are obtained via quadratic extrapolations as a function of  $1/L$ , as shown in Fig. 1. In all cases, we find that the phase factors in the sum rule and the sum rule itself are convergent in the thermodynamic limit. We also see that our edge-localized polarizations,  $\phi_{op/po}$ , have values similar to the other ones,  $\tilde{P}_{x/y}^{\text{edge}}$ , with differences at worst  $O(10^{-3})$ . In addition, when a  $C_4$  symmetry breaking term is small,  $\phi_{pp}$  has the same quantized value as the one predicted by the nested Wilson-loop approach [4]. Furthermore, the identification of  $\phi_{oo}$  with  $Q_c^{(2)}$  and the sum rule hold up to errors of  $O(10^{-4})$ . The errors may be attributed to the finite-size effect.

### 1. Quadrupole insulator $H_{\text{quad}}$

As our first model with the gapped Wannier spectrum, we consider the following tight-binding model [4] having a nonzero bulk quadrupole moment:

$$H_{\text{quad}}(\mathbf{k}) = [\gamma_x + \lambda_x \cos(k_x)]\Gamma_4 + \lambda_x \sin(k_x)\Gamma_3 + [\gamma_y + \lambda_y \cos(k_y)]\Gamma_2 + \lambda_y \sin(k_y)\Gamma_1 + \delta\Gamma_0, \quad (20)$$

where  $\Gamma_0 = \sigma_3 \otimes \sigma_0$ ;  $\Gamma_k = -\sigma_2 \otimes \sigma_k$  for  $k = 1, 2, 3$ ; and  $\Gamma_4 = \sigma_1 \otimes \sigma_0$  with  $\sigma_{k=1,2,3}$  being Pauli matrices and  $\sigma_0$  being the  $2 \times 2$  identity matrix.

When  $\delta = 0$ , there exist two anticommuting mirror symmetries which quantize the bulk quadrupole moment  $Q_{xy} = 0$  or  $1/2$ . The half-filled ground state of Eq. (20) realizes the topologically trivial quadrupole insulator when  $|\gamma_x| > |\lambda_x|$  and  $|\gamma_y| > |\lambda_y|$  and topologically nontrivial quadrupole insulator when  $|\gamma_x| < |\lambda_x|$  and  $|\gamma_y| < |\lambda_y|$ . When  $\delta \neq 0$ ,  $C_4$  symmetry and the mirror symmetries are broken and hence the bulk quadrupole moment is no longer quantized.

TABLE IV. The phase factors  $\phi_{ab}$  and the electric moments ( $Q_c^{(2)}$ ,  $\tilde{P}_x^{\text{edge}}$ ,  $\tilde{P}_y^{\text{edge}}$ ) are computed for the two band insulator  $H_{\text{two}}$  [Eq. (24)]. Here we use the same extrapolation procedure as in Table I. In this case as well, the edge-localized polarizations  $\tilde{P}_x^{\text{edge}}$  and  $\tilde{P}_y^{\text{edge}}$  agree with phase factors  $\phi_{po}$  and  $\phi_{op}$ , corner charge  $Q_c^{(2)}$  agrees with  $\phi_{oo}$ , and the sum rule is satisfied up to small errors.

Model parameters	Phase factors ( $\times 10^{-6}$ )				Electric moments ( $\times 10^{-6}$ )			Sum rule ( $\times 10^{-6}$ )
$H_{\text{two}}(t_1, t_2, t_3, t_4, t_5)$	$\phi_{pp}$	$\phi_{po}$	$\phi_{op}$	$\phi_{oo}$	$Q_c^{(2)}$	$\tilde{P}_x^{\text{edge}}$	$\tilde{P}_y^{\text{edge}}$	$\sum(-1)^{ab}\phi_{ab}$
(-2.2, -0.15, -0.1, -0.09, -0.06)	0.000(0)	1.459(0)	1.459(0)	2.920(0)	2.918(0)	0.851(0)	0.851(0)	0.002(0)

The numerical results for the quadrupole insulator are summarized in Table I.

### 2. Edge-localized polarization insulator $H_{\text{edge}}$

Our next model is the edge-localized polarization insulator [4]. The tight-binding Hamiltonian in the momentum space can be written as

$$H_{\text{edge}}(\mathbf{k}) = [\gamma_x + \lambda_x \cos(k_x)]\Gamma_4 + \lambda_x \sin(k_x)\Gamma_3 + [\gamma_y + \lambda_y \cos(k_y)]\tilde{\Gamma}_2 + \lambda_y \sin(k_y)\tilde{\Gamma}_1 + \delta\Gamma_0, \quad (21)$$

where  $\tilde{\Gamma}_2 = \sigma_1 \otimes \sigma_1$ ,  $\tilde{\Gamma}_1 = -\sigma_1 \otimes \sigma_2$ , and all the other  $\Gamma$  matrices are the same as the ones in Eq. (20).

The half-filled ground state of Eq. (21) has a vanishing bulk quadrupole moment but a nonzero corner charge. In particular, when  $\delta = 0$ , there exist two mirror symmetries  $M_x$  and  $M_y$  which quantize the corner charge to be 0 or  $1/2$ , where the corner charge is originated solely from the edge-localized polarizations [4]. The half-filled ground state of Eq. (21) with  $|\gamma_{x/y}| \ll |\lambda_{x/y}|$  has  $(\tilde{P}_x^{\text{edge}}, \tilde{P}_y^{\text{edge}}) = (0, 0.5)$  when  $\lambda_x > \lambda_y$  and  $(\tilde{P}_x^{\text{edge}}, \tilde{P}_y^{\text{edge}}) = (0.5, 0)$  when  $\lambda_x < \lambda_y$ .

The numerical results for the edge-localized polarization insulator are summarized in Table II.

### 3. Quadrupole insulator with $\pi/2$ flux per plaquette $H_{\text{quad}}^{(\pi/2)}$

Our third model is the quadrupole insulator with  $\pi/2$  flux per plaquette [20]. The tight-binding Hamiltonian in momentum space can be written as

$$H_{\text{quad}}^{(\pi/2)}(\mathbf{k}) = \gamma_x\Gamma_4 + \gamma_y(i\nu_2 \otimes \nu_2) + \delta\Gamma_0 - \lambda_x[\cos(k_x)(\sigma_y \otimes \sigma_0) + \sin(k_x)(\sigma_x \otimes \sigma_z)] - \lambda_y[\cos(k_y)(\nu_1 \otimes \nu_2) + \sin(k_y)(i\nu_1 \otimes \nu_1)], \quad (22)$$

TABLE V. The phase factors  $\phi_{ab}$  and the corner charge  $Q_c^{(2)}$  are computed for  $H_{2b}^{(4)}$  in Eq. (27) with various parameters. The number of filled electrons is taken as  $2N - 2$  with the number of sites  $N$  when the system is under the full open boundary condition due to the filling anomaly  $\eta = 2$ . Here we use the same extrapolation procedure as in Table I. The corner charge agrees with  $\phi_{oo}$  and the sum rule Eq. (14) is satisfied up to small errors.

Model parameters	Background	Phase factors				Electric moment	Sum rule
		$\phi_{pp}$	$\phi_{po}$	$\phi_{op}$	$\phi_{oo}$		
$H_{2b}^{(4)}(t, \delta)$	$\phi_0$					$Q_c^{(2)}$	$\sum(-1)^{ab}\phi_{ab}$
(0.1,0.001)	0.5	0.50000(0)	0.49992(0)	0.49992(0)	0.49983(0)	0.49983(0)	0.00000(0)
	0						
(0.1,0.1)	0.5	0.49972(0)	0.49433(0)	0.49433(0)	0.48896(0)	0.48895(0)	0.00002(0)
	0	0.49976(0)	0.49435(0)	0.49435(0)			
(0.1,0.5)	0.5	0.49732(2)	0.49095(1)	0.49095(1)	0.48461(0)	0.48460(0)	0.00003(0)
	0	0.49732(0)	0.49095(0)	0.49095(0)			0.00002(0)

where  $\nu_1$  and  $\nu_2$  are defined as

$$\nu_1 = \begin{bmatrix} 0 & 1 \\ i & 0 \end{bmatrix} \quad \text{and} \quad \nu_2 = \begin{bmatrix} 0 & 1 \\ -i & 0 \end{bmatrix}, \quad (23)$$

and all  $\Gamma$  and  $\sigma$  matrices are the same as in Eq. (20). Similar to the quadrupole insulator, which has  $\pi$  flux per plaquette, the bulk quadrupole moment of the half-filled ground state of Eq. (22) is quantized when  $\delta = 0$ . However, when  $\delta \neq 0$ , the bulk quadrupole moment  $Q_{xy}$  is nonzero and ( $Q_{xy}, P_{x/y}^{\text{edge}}, Q_c^{(2)}$ ) are *all* distinct unlike in the quadrupole insulator. These features provide nontrivial checks of the sum rule Eq. (14) and our observations Eqs. (15) and (19), which are summarized in Table III.

#### 4. Two band insulator $H_{\text{two}}$

Our final model is the two band insulator introduced in Ref. [33]. The tight-binding Hamiltonian in momentum space can be written as

$$H_{\text{two}}(\mathbf{k}) = \frac{t_1}{2}\sigma_1 + e^{ik_x} \begin{bmatrix} t_4 & t_2 \\ 0 & t_4 \end{bmatrix} + e^{ik_y} \begin{bmatrix} t_5 & t_3 \\ 0 & t_5 \end{bmatrix} + \text{H.c.}, \quad (24)$$

with the five hopping parameters ( $t_1, t_2, t_3, t_4, t_5$ ). The half-filled ground state of this Hamiltonian has nonzero corner charge and edge-localized polarizations.

The numerical results for the two band insulator with the same parameters as in Ref. [33] are summarized in Table IV.

TABLE VI. The phase factors  $\phi_{ab}$  and the corner charge  $Q_c^{(2)}$  are computed for  $H_{1b}^{(4)} \oplus H_{2c}^{(4)}$  in Eq. (28) with various parameters. On each  $\phi_0$ , all observables are obtained by extrapolating them as a function of  $1/\sqrt{L_x L_y}$ . The phase factors  $\phi_{ab}$  converge to different values on each  $\phi_0$ , so we separate the convergence values of  $\phi_{ab}$  by each value of  $\phi_0$ . Each extrapolation uses a sequence of four system sizes with the interval  $(\Delta L_x, \Delta L_y) = (4, 4)$ , and each sequence starts from  $(L_x, L_y) = (18, 16), (18, 17), (18, 18)$ , and  $(19, 19)$ , which correspond to  $\phi_0 = -0.25, 0.5, 0.25$ , and  $0$ , respectively. Here, we use the same extrapolation procedure as in Table I. The corner charge agrees with  $\phi_{oo}$  and the sum rule Eq. (14) is satisfied up to small errors.

Model parameters	Background	Phase factors				Electric moment	Sum rule
		$\phi_{pp}$	$\phi_{po}$	$\phi_{op}$	$\phi_{oo}$		
$H_{1b}^{(4)} \oplus H_{2c}^{(4)}(t_x, t_y, t)$	$\phi_0$					$Q_c^{(2)}$	$\sum(-1)^{ab}\phi_{ab}$
(0,0,0.1)	-0.25	0.33354(0)	-0.33994(1)	-0.07653(1)	0.24992(1)	0.25000(0)	-0.00007(1)
	0.5	0.14434(1)	-0.49995(1)	-0.10573(0)	0.24997(0)		-0.00002(0)
	0.25	0.43112(2)	-0.15944(1)	-0.15944(1)	0.24999(0)		0.00000(0)
	0	-0.24983(2)	-0.49992(1)	-0.49992(1)	0.24999(0)		0.00000(0)
(0.1,0.1,0.1)	-0.25	0.374(2)	-0.307(1)	-0.0683(3)	0.24992(1)	0.25000(0)	-0.00007(1)
	0.5	0.1592(5)	0.49999(0)	-0.0908(5)	0.24997(0)		-0.00002(0)
	0.25	0.489(2)	-0.131(1)	-0.131(1)	0.24999(0)		0.00000(0)
	0	-0.24984(2)	-0.49992(1)	-0.49992(1)	0.24999(0)		0.00000(0)
(0.01,0.1,0.1)	-0.25	0.33455(4)	-0.33916(4)	-0.07630(0)	0.24992(1)	0.25000(0)	-0.00007(1)
	0.5	0.14470(1)	0.49999(0)	-0.10530(1)	0.24997(0)		-0.00002(0)
	0.25	0.43274(8)	-0.15863(4)	-0.15863(4)	0.24999(0)		0.00000(0)
	0	-0.24983(2)	-0.49992(1)	-0.49992(1)	0.24999(0)		0.00000(0)

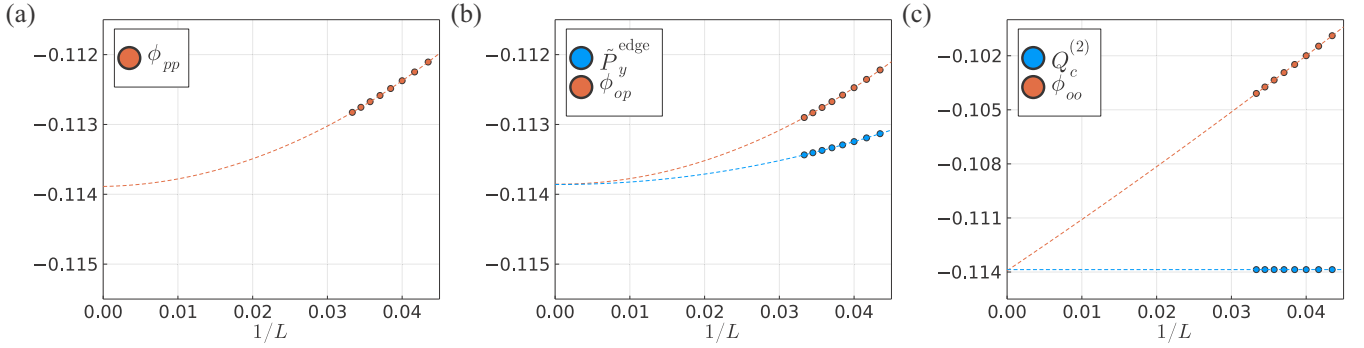


FIG. 1. (a–c) Extrapolation of the observables (a)  $\phi_{pp}$ , (b)  $\phi_{op}$  and  $\tilde{P}_y^{\text{edge}}$ , and (c)  $\phi_{oo}$  and  $Q_c^{(2)}$ , as a quadratic function in  $1/L$  for the quadrupole insulator [Eq. (20)] with parameters  $(\gamma_x, \gamma_y, \lambda_x, \lambda_y, \delta) = (0.5, 0.5, 1.0, 1.0, 0.7)$  and isotropic system sizes. The quadratic extrapolation works well and the error from the extrapolation is less than  $10^{-5}$  in all cases. (b)  $\phi_{op}$  and  $\tilde{P}_y^{\text{edge}}$  agree with each other in  $O(10^{-5})$ . (c)  $\phi_{oo}$  and  $Q_c^{(2)}$  agree with each other in the same order of accuracy.

## B. Models with the hybrid Wannier value at 0.5

We now turn to models with the hybrid Wannier value at 0.5, which are all based on  $C_4$ -symmetric insulators [24]. Note that for the models presented below, a HWF with the corresponding hybrid Wannier value at 0.5 exists even after introducing a  $C_4$  symmetry breaking term. In these models, corner charges are originated from the filling anomaly  $\eta$  [24]:

$$\eta = \text{no. ions} - \text{no. electrons} \pmod{4}, \quad (25)$$

where the number of ions equals the number of lattice sites times the filling. In each model, we take into account the filling anomaly  $\eta$  which determines the corner charge and the phase factor  $\phi_{oo}$ , where we tune the chemical potential to include or not include the zero modes in the full open boundary conditions.

For tested models which are specified below, we numerically compute the phase factors  $\phi_{ab}$  [Eq. (13)] and the corner charge  $Q_c^{(2)}$  [Eq. (11)]. The results are summarized in Tables V and VI. In the tables,  $\tilde{P}_{x/y}^{\text{edge}}$  are not presented since they depend sensitively on the choice of the branch cut for the considered models, as we discuss in Appendix F. However, we do compare the corner charge  $Q_c^{(2)}$  with  $\phi_{oo}$  and check whether the sum rule Eq. (14) is satisfied. All observables in the tables are the extrapolated values in the thermodynamic limit as described in Sec. III A.

For each model, we separate the cases based on the quadrupole moment  $\phi_0$  of the background ions:

$$\phi_0 \equiv -n_e(L_x + 1)(L_y + 1)/4 \pmod{1}, \quad (26)$$

with  $n_e$  being the charge of the ions at each lattice site and  $(L_x, L_y)$  being the linear system sizes. We then obtain  $\phi_{ab}$  and  $Q_c^{(2)}$  in the thermodynamic limit  $L \rightarrow \infty$  for each value of  $\phi_0$  and summarize the numerical results in Tables V and VI. We find that for the model Eq. (28) defined below, the convergent values of the three phase factors  $\phi_{pp}$ ,  $\phi_{op}$ , and  $\phi_{po}$  depend on  $\phi_0$  while the phase factor  $\phi_{oo}$  is convergent on the same model. In contrast, all the phase factors are convergent on the other

model Eq. (27). Thus, at least  $\phi_{oo}$  is interpretable among the four phase factors for these models. In addition, we find that in all cases,  $\phi_{oo}$  converges to corner charge  $Q_c^{(2)}$  up to an error  $O(10^{-5})$ , and the sum rule holds up to the same order of an error.

### 1. $C_4$ -symmetric insulator $H_{2b}^{(4)}$

We first consider a  $C_4$ -symmetric insulator  $H_{2b}^{(4)}$  introduced in Ref. [24] with a  $C_4$  symmetry breaking term parametrized by  $\delta$ :

$$H_{2b}^{(4)}(\mathbf{k}) = \begin{bmatrix} \delta & t & e^{i(k_x+k_y)} & t \\ t & -\delta & t & e^{-i(k_x-k_y)} \\ e^{-i(k_x+k_y)} & t & \delta & t \\ t & e^{i(k_x-k_y)} & t & -\delta \end{bmatrix}. \quad (27)$$

When  $\delta = 0$  and  $t < 1$ , the half-filled ground state of Eq. (27) respects  $C_4$  symmetry and has filling anomaly  $\eta = 2$ . Therefore, on full open boundary conditions, filling  $2N - 2$  electrons, where  $N$  is the number of sites, results in the corner charge of  $-1/2$  (in the unit of electron charge) at each corner. When  $\delta \neq 0$ , the ground state no longer respects  $C_4$  symmetry and the corner charge is not quantized.

The numerical results for the  $C_4$ -symmetric insulator  $H_{2b}^{(4)}$  are summarized in Table V.

### 2. $C_4$ -symmetric insulator $H_{1b}^{(4)} \oplus H_{2c}^{(4)}$

Finally, we consider the  $C_4$ -symmetric insulator [24]  $H_{1b}^{(4)} \oplus H_{2c}^{(4)}$ . This model was used as an example in which  $\phi_{pp}$  depends on the system size [22], which indicates it is ill defined on this model. We also see that  $\phi_{pp}$  in fact does as discussed below. The tight-binding Hamiltonian of this model in the momentum space is given by

$$H_{1b}^{(4)} \oplus H_{2c}^{(4)}(\mathbf{k}) = \begin{bmatrix} H_{1b}^{(4)} & \gamma^{(4)}(t) \\ \gamma^{(4)}(t)^\dagger & H_{2c}^{(4)} \end{bmatrix}, \quad (28)$$

where

$$H_{1b}^{(4)}(\mathbf{k}) = \begin{bmatrix} 0 & t_x + e^{ik_x} & 0 & t_y + e^{ik_y} \\ t_x + e^{-ik_x} & 0 & t_y + e^{ik_y} & 0 \\ 0 & t_y + e^{-ik_y} & 0 & t_x + e^{-ik_x} \\ t_y + e^{-ik_y} & 0 & t_x + e^{ik_x} & 0 \end{bmatrix}, \quad H_{2c}^{(4)}(\mathbf{k}) = \begin{bmatrix} 0 & 0 & t_x & 0 \\ 0 & 0 & 0 & t_y \\ t_x & 0 & 0 & 0 \\ 0 & t_y & 0 & 0 \end{bmatrix} + 1.5 \begin{bmatrix} 0 & 0 & e^{ik_x} & 0 \\ 0 & 0 & 0 & e^{ik_y} \\ e^{-ik_x} & 0 & 0 & 0 \\ 0 & e^{-ik_y} & 0 & 0 \end{bmatrix},$$

and

$$\gamma^{(4)}(t) = \begin{bmatrix} t & t & 0 & 0 \\ 0 & t & t & 0 \\ 0 & 0 & t & t \\ t & 0 & 0 & t \end{bmatrix}.$$

Both the  $1/4$ -filled ground state of  $H_{1b}^{(4)}$  and the  $1/2$ -filled ground state of  $H_{2c}^{(4)}$  have nonzero bulk polarizations, and we stack two models and introduce an additional hopping term given by  $\gamma^{(4)}(t)$  so that the  $3/8$ -filled ground state of the stacked model has vanishing bulk polarization while respecting  $C_4$  symmetry. The stacked model  $H_{1b}^{(4)} \oplus H_{2c}^{(4)}$  has the filling anomaly  $\eta = 3$  which results in  $-3/4$  corner charge (in the unit of electron charge) at each corner when  $4N - 3$  electrons are filled under full open boundary conditions, where  $N$  is the number of sites.

The numerical results for the  $C_4$ -symmetric insulator  $H_{1b}^{(4)} \oplus H_{2c}^{(4)}$  are summarized in Table VI.

#### IV. CONCLUSION

In this paper, we have presented the bulk-boundary correspondence for the bulk quadrupole moment which is expressed in terms of the phase factors of the expectation values of the many-body operators with respect to the ground states under various boundary conditions. Our bulk-boundary correspondence is given by the cancellation between the four gauge-invariant phase factors, which can be computed in fully interacting systems. We also have proposed that one of them is expected to be identified with the corner charge. On these, we have numerically observed that when the band insulator is without the hybrid Wannier value at 0.5, each phase factor corresponds to a physical observable including the bulk multipole moment and edge-localized polarizations. Whether the same correspondence holds with the hybrid Wannier value at 0.5 has not been fully understood yet. Through extensive numerical computations on band insulators, we have found that our bulk-boundary correspondence and the identification of one of the phase factors with the corner charge hold up to small errors of  $O(10^{-4})$ , which might be originated from the finite-size effect of the numerics. Furthermore, we have also found that another two of the phase factors have values similar to the edge-localized polarizations defined in Ref. [4] with differences at most  $O(10^{-3})$ , which supports our observations.

Let us conclude by making remarks on possible future directions of our work. It would be interesting to prove the sum rules at least in the case of band insulators. This would also extend our knowledge of bulk multipole moments in solids. Comparing our definition of the quadrupole moment with another one proposed in Ref. [34] would be interesting. Since our formulation works for disordered and interacting systems, one could also test our sum rules for those cases. Finally, finding connections between previous works [29–31] and our sum rule would be interesting.

#### ACKNOWLEDGMENTS

W.L. and G.Y.C. acknowledge the support of the National Research Foundation of Korea (NRF) funded by the Korean Government (Grants No. 2020R1C1C1006048, No.

2020R1A4A3079707). W.L. and G.Y.C. also acknowledge the support by IBS-R014-D1. This work is also supported by the U.S. Air Force Office of Scientific Research under Grant No. FA2386-20-1-4029. B.K. is supported by KIAS individual Grant No. PG069402 at Korea Institute for Advanced Study and a NRF grant funded by the Korean government (Grant No. 2020R1F1A1075569). G.Y.C. acknowledges financial support from Samsung Science and Technology Foundation under Project No. SSTF-BA2002-05.

#### APPENDIX A: CLASSICAL MULTIPOLAR SUM RULES

In this Appendix, we derive classical dipolar and quadrupolar sum rules based on classical electrostatics. The derivations closely follow the construction presented in Ref. [4]. Here, we consider continuum systems for classical systems.

##### 1. Classical dipolar sum rule

The macroscopic polarization  $\vec{P}(\vec{R})$  is defined in the classical electrostatics as the averaged first moment of the charge density over a region  $v(\vec{R})$ , which is small compared with the whole system:

$$\vec{P}(\vec{R}) = \frac{1}{|v(\vec{R})|} \int_{v(\vec{R})} d^3r \rho(\vec{r} + \vec{R}) \vec{r}, \quad (\text{A1})$$

where  $\rho(\vec{r})$  is the volume charge density and  $|v(\vec{R})|$  is the volume of the region  $v(\vec{R})$ . It is well known that a macroscopic system with the bulk polarization  $\vec{P}$  induces the charge density  $\rho$  via

$$\rho = -\nabla \cdot \vec{P}. \quad (\text{A2})$$

Suppose that the system has a boundary to the vacuum so that the polarization drops on the boundary; then the boundary charge  $Q_c$  is accumulated on the boundary:

$$Q_c = - \int_v \nabla \cdot \vec{P} dv = - \oint_{\partial v} \vec{P} \cdot d\vec{s}, \quad (\text{A3})$$

where  $\partial v$  is the boundary of a volume  $v$  which encircles the boundary of the system as shown in Fig. 2, and  $\vec{s}$  is the surface vector normal to  $\partial v$ . If the system is one-dimensional and has a uniform bulk polarization density  $\mathcal{P}$  along the  $x$  direction, then Eq. (A3) becomes

$$Q_c = \mathcal{P}, \quad (\text{A4})$$

which is depicted in Fig. 2, with the circle containing the plus symbol being the boundary charge.

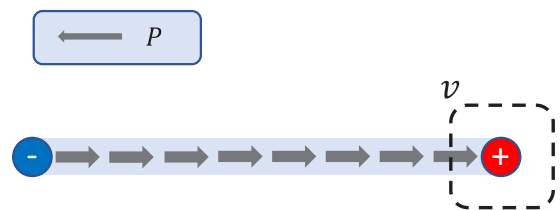


FIG. 2. A schematics of the polarization in a one-dimensional system. Here, gray arrows represent the bulk polarization. The bulk polarization  $\mathcal{P}$  accumulates charges at each boundary with the same amount but different signs.

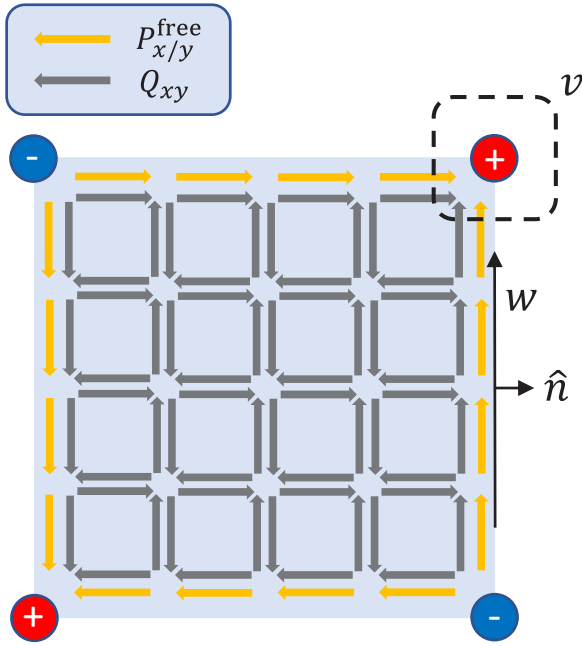


FIG. 3. Schematic understanding of the bulk quadrupole moment and the free edge polarization. Here, gray arrows and orange arrows represent the quadrupole moment and the free edge polarization, respectively. Both of them accumulate charges at each corner, and the total amount of charge at each corner is fixed by the charge conservation law Eq. (A7).

## 2. Classical quadrupolar sum rule

The macroscopic quadrupole moment  $Q_{ij}(\vec{R})$  is defined in the classical electrostatics as the averaged second moment of the charge density over  $v(\vec{R})$ :

$$Q_{ij}(\vec{R}) = \frac{1}{|v(\vec{R})|} \int_{v(\vec{R})} d^3r \rho(\vec{r} + \vec{R}) r_i r_j, \quad (\text{A5})$$

where  $\rho(\vec{r})$  is the volume charge density. We first consider a classical system with a uniform bulk quadrupole moment  $Q_{ij}$ . We assume that the system has a vanishing bulk polarization, which follows when the system has inversion symmetry. Then the quadrupole moment  $Q_{ij}$  induces the charge density  $\rho$  via

$$\rho = \frac{1}{2} \sum_{i,j} \partial_i \partial_j Q_{ij}. \quad (\text{A6})$$

If we consider a rectangular geometry as in Fig. 3, then the corner charge  $Q_c$  accumulated on a corner of a macroscopic two-dimensional system due to quadrupole moment  $Q_{ij}$  drop is given by

$$Q_c = \frac{1}{2} \sum_{i,j} \int_v \partial_i \partial_j Q_{ij} dv = \frac{1}{2} \sum_{i,j} \oint_{\partial v} \partial_i Q_{ij} n_j ds, \quad (\text{A7})$$

where  $n_i$  is the  $i$ th component of the unit vector normal to  $\partial v$ ,  $v$  is a volume enveloping the corner, and  $\partial v$  is the boundary of  $v$ , which are illustrated in Fig. 3. For a rectangular system, Eq. (A7) becomes

$$Q_c = Q_{xy}, \quad (\text{A8})$$

where we used the symmetry of the quadrupole moment,  $Q_{xy} = Q_{yx}$ . In addition to inducing corner charge, the quadrupole moment also induces the polarizations along the edges, which we call the edge-localized polarizations. To this end, we first consider the geometry given in Fig. 3. The line charge density  $\sigma_w$  at the edge  $w$  in Fig. 3 is given as

$$\sigma_w = - \sum_{i,j} \partial_j (n_i Q_{ij}), \quad (\text{A9})$$

where  $n_i$  is the normal vector of the edge in Fig. 3. Since the charge density is given as the divergence of  $\sum_i n_i Q_{ij}$ , this can be considered as the polarization induced by the quadrupole moment localized on the edge  $w$ . We will call this polarization as  $\mathcal{P}_n^{\text{quad}}$ . For a rectangular system, the quadrupole induced polarizations at the  $y$  boundaries  $\mathcal{P}_x^{\text{quad}}$  and the  $x$  boundaries  $\mathcal{P}_y^{\text{quad}}$  are given by

$$\mathcal{P}_x^{\text{quad}} = \mathcal{P}_y^{\text{quad}} = Q_{xy}. \quad (\text{A10})$$

On the other hand, one can dress one-dimensional systems having edge polarizations  $\mathcal{P}_x^{\text{free}}$  and  $\mathcal{P}_y^{\text{free}}$  along the boundaries while respecting the inversion symmetry, where  $\mathcal{P}_x^{\text{free}}$  and  $\mathcal{P}_y^{\text{free}}$  do not come from the quadrupole moment. Note that  $\mathcal{P}_{x/y}^{\text{free}}$  also accumulates the charge  $Q_c^{\text{free}}$  at the corner due to the dipolar sum rule:

$$Q_c^{\text{free}} = \mathcal{P}_x^{\text{free}} + \mathcal{P}_y^{\text{free}}. \quad (\text{A11})$$

Thus, if we define the edge-localized polarization  $\mathcal{P}_{x/y}^{\text{edge}}$  in classical systems as

$$\mathcal{P}_{x/y}^{\text{edge}} \equiv \mathcal{P}_{x/y}^{\text{quad}} + \mathcal{P}_{x/y}^{\text{free}}, \quad (\text{A12})$$

then the corner charge is given by

$$Q_c = -Q_{xy} + \mathcal{P}_x^{\text{edge}} + \mathcal{P}_y^{\text{edge}}. \quad (\text{A13})$$

We call Eq. (A13) the quadrupolar sum rule in classical systems, which is summarized in Fig. 3.

## APPENDIX B: FIELD THEORETIC DERIVATIONS OF $\phi_{ab}$

Here, we show that the phase factors  $\phi_{pp}$ ,  $\phi_{op/po}$ , and  $\phi_{oo}$  should correspond to quadrupole moment  $Q_{xy}$ , edge-localized polarization  $\mathcal{P}_{y/x}^{\text{edge}}$ , and corner charge  $Q_c$  in the thermodynamic limit. To see these, we closely follow the effective field theory description of the multipoles elaborated in Ref. [20].

We first briefly summarize the effective field theory description of the phase factors  $\phi_{ab}$  [20]. We start from the thermal expectation of an operator  $\hat{U}_a(\vec{r}) = e^{i\phi_a(\vec{r})\hat{n}(\vec{r})}$ :

$$\langle \hat{U}_a \rangle_\beta = \frac{1}{Z} \text{Tr}[e^{-\beta\hat{H}} \hat{U}_a] \quad (\text{B1})$$

with the partition function  $Z = \text{Tr}[e^{-\beta\hat{H}}]$ . The ground-state expectation value of  $\hat{U}_a$  can be achieved in the limit of  $\beta \rightarrow \infty$ ,

$$\langle \text{GS} | \hat{U}_a | \text{GS} \rangle = \lim_{\beta \rightarrow \infty} \langle \hat{U}_a \rangle_\beta, \quad (\text{B2})$$

or equivalently, we can rewrite it as

$$\langle \text{GS} | \hat{U}_a | \text{GS} \rangle = \frac{1}{Z} \text{Tr}[e^{-\int_0^\infty \int_{\mathcal{M}} d\tau d^2r [\hat{H} - i\phi_a \hat{n} \delta(\tau)]}], \quad (\text{B3})$$

where  $\mathcal{M}$  is a region we considered. The right-hand side of Eq. (B3) except  $1/Z$  can be interpreted as the partition function of a system coupled with the gauge potential  $A_0(\vec{r}, \tau) = \phi_a(\vec{r})\delta(\tau)$ . Performing the trace in the above expression, i.e., integrating out the fermionic degrees of freedom of the right-hand side, we find

$$\frac{1}{2\pi} \text{Im} \log \langle \text{GS} | \hat{U}_a | \text{GS} \rangle = \frac{1}{2\pi} S_{\text{eff}}[A_0(\vec{r}, \tau)] \pmod{1}.$$

For more details to derive this result, we refer to Refs. [20,35–37]. To proceed, we note that the electric response of insulators can be naturally expanded by electric multipoles in the region  $\mathcal{M}$ . Here, the insulators that we consider do not have the Chern numbers. For the case with the Chern number, please see Refs. [38,39]. Hence we expect [20]

$$\begin{aligned} S_{\text{eff,monopole}} &= \int_0^\infty \int_{\mathcal{M}} d\tau d^2r \rho A_0, \\ S_{\text{eff,dipole}} &= \int_0^\infty \int_{\mathcal{M}} d\tau d^2r \vec{P} \cdot \vec{E}, \\ S_{\text{eff,quadrupole}} &= \int_0^\infty \int_{\mathcal{M}} d\tau d^2r \frac{Q_{xy}}{2} [\partial_x E_y + \partial_y E_x]. \end{aligned}$$

Using these effective actions, we can demonstrate that the phase factors  $\phi_{pp}$ ,  $\phi_{op/po}$ , and  $\phi_{oo}$  indeed correspond to quadrupole moment, edge-localized polarization, and corner charge in the thermodynamic limit.

### 1. Interpretation of $\phi_a$

Before giving the derivations of  $\phi_{ab}$ , we illustrate that the effective action approach correctly predicts the identifications of  $\phi_p$  with polarization as well as  $\phi_o$  with boundary charge, which is shown in Ref. [18] and Appendix C, respectively. For these, we will set  $\hat{U}_a$  as Resta's  $\hat{U}_1$  operator [18]:

$$\hat{U}_1(x) = \exp \left[ \frac{2\pi i}{L_x} x \right], \quad (\text{B4})$$

so we have  $A_0[x, \tau] = \frac{2\pi}{L_x} x \delta(\tau)$  and  $E_x = \frac{2\pi}{L_x} \delta(\tau)$ .

First, we can show that  $\phi_p$  corresponds to polarization, which reproduces Resta's formula. We consider a line  $\mathcal{M} = (0, L_x)$  having constant polarization  $P_x$  and periodic boundaries. Then, the effective action of the region  $\mathcal{M}$  is given by

$$S_{\text{eff},p} = \int_0^\infty \int_{\mathcal{M}} d\tau dx P_x E_x. \quad (\text{B5})$$

Then, inserting the gauge potential  $A_0$  to the effective action gives

$$S_{\text{eff},p} = \frac{2\pi}{L_x} \int_{\mathcal{M}} dx P_x = 2\pi P_x, \quad (\text{B6})$$

so we have

$$\phi_p = P_x \pmod{1}. \quad (\text{B7})$$

Next, we can show that  $\phi_o$  corresponds to the boundary charge, when the system is subject to the open boundary conditions. In this case, we consider the same  $\mathcal{M}$  having constant polarization  $P$  as well as free boundary charge  $Q_c^{\text{free}}$ , i.e., free

electrons which can be added and are not related to the bulk polarization, and open boundaries. Then, the effective action is

$$S_{\text{eff},o} = \int_0^\infty \int_{\mathcal{M}} d\tau dx \{ P_x E_x + Q_c^{\text{free}} A_0 [\delta(x - L_x) + \delta(x)] \}.$$

Again, inserting the gauge potential to the effective action gives

$$S_{\text{eff},p} = 2\pi (P_x + Q_c^{\text{free}}), \quad (\text{B8})$$

so we have

$$\phi_o = P_x + Q_c^{\text{free}} \pmod{1}, \quad (\text{B9})$$

where the right-hand side is the boundary charge predicted by the classical electrostatics.

From these, we can also easily show the bulk-boundary correspondence in terms of the phase factors. Since  $Q_c^{\text{free}}$  is an integer, we have

$$\phi_p = \phi_o \pmod{1}. \quad (\text{B10})$$

### 2. Interpretation of $\phi_{ab}$

We then give the derivations of  $\phi_{ab}$  for two-dimensional systems using the effective field theory approach. To do so, we will consider a square region  $\mathcal{M} = (0, L_x) \times (0, L_y)$  with an inversion symmetric Hamiltonian for all cases; however, the boundary conditions of  $\mathcal{M}$  will be chosen differently for each case.

We first discuss the identification of  $\phi_{pp}$  with  $Q_{xy}$ . Let the region  $\mathcal{M}$  have periodic boundaries along the  $x$  and  $y$  directions and assume that the region has constant quadrupole moment and vanishing polarizations. In addition, since we deal with  $\hat{U}_2$ , we set the gauge potential as  $A_0[\vec{r}, \tau] = \frac{2\pi}{L_x L_y} xy \delta(\tau)$ . Then, the effective action of the region  $\mathcal{M}$  is given by

$$S_{\text{eff},pp} = \int_0^\infty \int_{\mathcal{M}} d\tau d^2r \frac{1}{2} Q_{xy} [\partial_x E_y + \partial_y E_x]. \quad (\text{B11})$$

Thus, inserting the gauge potential to the effective action gives

$$S_{\text{eff},pp} = \frac{2\pi}{L_x L_y} \int_{\mathcal{M}} d^2r Q_{xy} = 2\pi Q_{xy}. \quad (\text{B12})$$

In other words,  $\langle \text{GS} | \hat{U}_a | \text{GS} \rangle$  is proportional to  $e^{2\pi i Q_{xy}}$ , so we can identify  $\phi_{pp}$  with  $Q_{xy}$ .

We next discuss the identification of  $\phi_{op}$  with  $P_y^{\text{edge}}$ . In this case, we let the region have open boundaries along the  $x$  direction and periodic boundaries along the  $y$  direction and assume that the region has constant quadrupole moment as well as constant free edge-localized polarizations  $P_y^{\text{free}}$  along the opened boundaries that respect inversion symmetry, i.e.,  $P_y^{\text{free}}$  is not related to the bulk quadrupole moment. One example of this is the edge polarization model [4]. Then, the effective action is given as

$$\begin{aligned} S_{\text{eff},op} &= \int_0^\infty \int_{\mathcal{M}} d\tau d^2r \left\{ \frac{1}{2} Q_{xy} [\partial_x E_y + \partial_y E_x] \right. \\ &\quad \left. + P_y^{\text{free}} E_y [\delta(x - L_x) - \delta(x)] \right\}. \end{aligned} \quad (\text{B13})$$

Again, inserting the gauge potential to the effective action gives

$$\begin{aligned} S_{\text{eff},op} &= \frac{2\pi}{L_x L_y} \int_{\mathcal{M}} d^2 r \{ Q_{xy} + P_y^{\text{edge}} x [\delta(x - L_x) - \delta(x)] \} \\ &= 2\pi (Q_{xy} + P_y^{\text{free}}). \end{aligned}$$

Thus, we have  $\phi_{op} = Q_{xy} + P_y^{\text{free}} \pmod{1}$ . As we discussed in Appendix A, the total edge-localized polarization  $P_y^{\text{edge}}$  is given by the sum of the free edge-localized polarization  $P_y^{\text{free}}$  and the quadrupole induced edge-localized polarization, which is  $Q_{xy}$  for square systems. Therefore, we can identify  $\phi_{op}$  with the edge-localized polarization  $P_y^{\text{edge}}$ . In the same fashion,  $\phi_{po}$  should be identified with  $P_x^{\text{edge}}$ .

We finally discuss the identification of  $\phi_{oo}$  with  $Q_c$ . In this case, we let the region have full open boundaries and assume that the region has constant  $Q_{xy}$ , constant  $P_{x/y}^{\text{free}}$ , and free corner charge  $Q_c^{\text{free}}$ . Again, we will assume that the system has inversion symmetry. These assumptions give the effective action as

$$\begin{aligned} S_{\text{eff},oo} &= \int_0^\infty \int_{\mathcal{M}} d\tau d^2 r \left\{ \frac{1}{2} Q_{xy} [\partial_x E_y + \partial_y E_x] \right. \\ &\quad + P_y^{\text{free}} E_y [\delta(x - L_x) - \delta(x)] \\ &\quad + P_x^{\text{free}} E_x [\delta(y - L_y) - \delta(y)] \\ &\quad + Q_c^{\text{free}}(x, y) A_0 [\delta(x - L_x) \delta(y - L_y) + \delta(x) \delta(y) \\ &\quad \left. - \delta(x) \delta(y - L_y) - \delta(x - L_x) \delta(y)] \right\} \quad (\text{B14}) \end{aligned}$$

with  $Q_c^{\text{free}}(0, 0) = Q_c^{\text{free}}(L_x, L_y)$  and  $Q_c^{\text{free}}(L_x, 0) = Q_c^{\text{free}}(0, L_y)$ . Then, the insertion of the gauge potential to the effective action gives

$$\phi_{oo} = Q_{xy} + P_x^{\text{free}} + P_y^{\text{free}} + Q_c^{\text{free}}(L_x, L_y) \pmod{1}.$$

One can see using the classical electrostatics that the right-hand side is indeed the corner charge at  $\vec{r} = (L_x, L_y)$ , and so is  $\phi_{oo}$ .

We can also directly derive the quadrupole sum rule using the above results. Since the free corner charge  $Q_c^{\text{free}}(L_x, L_y)$  is an integer, we have

$$\phi_{pp} + \phi_{oo} = \phi_{op} + \phi_{po} \pmod{1}. \quad (\text{B15})$$

In summary, the sum rule and the identifications of the quadrupole moment, edge-localized polarizations, and corner charge can be justified via the above effective field theory descriptions of multipoles.

### APPENDIX C: $\hat{U}_1$ OPERATOR AND THE CORNER CHARGE

In this Appendix, we show that for band insulators in one dimension, the phase factor of the  $\hat{U}_1$  expectation value with respect to the ground state in the open boundary condition converges to the boundary charge in the thermodynamic limit.

We prove the claim by constructing bulk and boundary Wannier functions. The bulk Wannier functions are identical to the Wannier functions in the periodic boundary condition and the boundary Wannier functions are localized near the left and right boundaries. The phase factor of the  $\hat{U}_1$  expectation value is determined by the bulk Wannier functions

while boundary Wannier functions do not contribute, as in the original bulk-boundary correspondence for the polarization [17,23]. To avoid any ambiguity, we assume that no mode exists at the chemical potential, which can always be done by either introducing a (small) symmetry breaking term splitting the zero modes or tuning the chemical potential slightly.

In the open boundary condition, the position operator  $\hat{x}$  is well defined, which we choose to take values in  $\{1, 2, \dots, L\}$ , and thus we can diagonalize the position operator in the subspace of occupied single-particle orbitals  $P_{\text{occ}}$ . We would like to show that the eigenvectors of  $P_{\text{occ}}(\hat{x})P_{\text{occ}}$  are exactly the bulk and boundary Wannier functions with desirable properties.

We first recall the results in Refs. [14,40], which state that the Wannier functions  $\{|w_{\alpha,R}\rangle\}$ , where  $\alpha = 1, \dots, n_e$  with  $n_e$  being the electron filling and  $R \in \mathbb{Z}$  labeling the position at which the Wannier function is localized, are the eigenvectors of the  $\hat{x}$  operator in the subspace of the occupied single-particle orbitals of the *infinite* open system with the corresponding eigenvalues  $R + v_\alpha$ . At the same time,  $\{|w_{\alpha,R}\rangle\}$  are the eigenvectors of  $e^{\frac{2\pi i \hat{x}}{L}}$  in the subspace of occupied single-particle orbitals of a periodic system with the corresponding eigenvalues  $e^{i2\pi(R+v_\alpha)/L}$ , when the system size  $L$  is sufficiently large. Moreover, the Wannier functions  $\{|w_{\alpha,R}\rangle\}$  are exponentially localized and satisfy the usual property  $\langle x | w_{\alpha,R+1} \rangle = \langle x - 1 | w_{\alpha,R} \rangle$ .

Let us take a positive integer  $\delta$  which is much larger than the localization lengths of  $\{|w_{\alpha,R}\rangle\}$ . Using the exponentially localized nature,  $\{|w_{\alpha,R}\rangle\}_{R=\delta+1, \delta_2, \dots, L-\delta}$  are the claimed bulk Wannier functions, i.e., eigenvectors of  $P_{\text{occ}}(\hat{x})P_{\text{occ}}$  localized on the bulk, where  $P_{\text{occ}}$  projects to the subspace of occupied single-particle orbitals of a finite open system. Also, for a sufficiently large  $L$ , the bulk Wannier functions  $\{|w_{\alpha,R}\rangle\}_{R=\delta+1, \delta_2, \dots, L-\delta}$  are the eigenvectors of  $P_{\text{occ}}(e^{\frac{2\pi i \hat{x}}{L}})P_{\text{occ}}$  with the corresponding eigenvalues  $e^{i2\pi(R+v_\alpha)/L}$ . The remaining eigenvectors of  $P_{\text{occ}}(\hat{x})P_{\text{occ}}$  are localized near the left and right boundaries, hence we call them the boundary Wannier functions.

We now evaluate the expectation value of  $\hat{U}_1$  using the bulk and boundary Wannier functions. Since the ground state of a band insulator is given by the Slater determinant of occupied single-particle orbitals, which we choose to be the bulk and boundary Wannier functions,  $\langle \hat{U}_1 \rangle$  can be expressed as

$$\langle \hat{U}_1 \rangle = e^{-(L+1)n_e \pi i} \det \left[ \begin{pmatrix} \mathcal{L} & 0 & 0 \\ 0 & \mathcal{D} & 0 \\ 0 & 0 & \mathcal{R} \end{pmatrix} \right], \quad (\text{C1})$$

where  $e^{-(L+1)n_e \pi i}$  is the phase factor from background ions,  $\mathcal{L}$  and  $\mathcal{R}$  are  $n_e \delta$ -by- $n_e \delta$  matrices, and

$$\mathcal{D} = \text{diag} \left( e^{2\pi i \frac{\delta+1+v_1}{L}}, \dots, e^{2\pi i \frac{L-\delta+v_{n_e}}{L}} \right) \quad (\text{C2})$$

is a diagonal matrix. By expanding the diagonal part in the determinant, we get

$$\begin{aligned} \langle U_1 \rangle &= e^{-(L+1)n_e \pi i} e^{\frac{2\pi i}{L} \left( \frac{(L+1)(L-2\delta)}{2} n_e + L \sum_{\alpha=1}^{n_e} v_\alpha \right)} \det(\mathcal{L}) \det(\mathcal{R}) \\ &= e^{2\pi i \frac{L+1}{L} (-\delta)} e^{2\pi i \sum_{\alpha=1}^{n_e} v_\alpha} \det(\mathcal{L}) \det(\mathcal{R}) \\ &= e^{-2\pi i \frac{\delta}{L}} e^{2\pi i \sum_{\alpha=1}^{n_e} v_\alpha} \det(\mathcal{L}) \det(\mathcal{R}), \quad (\text{C3}) \end{aligned}$$

where we used the fact that  $\delta$  is an integer in the last equality. Note that  $\mathcal{L}$  ( $\mathcal{R}$ ) is the matrix representation of  $e^{\frac{2\pi i x}{L}}$  with respect to the left (right) Wannier functions which are localized within the range  $\delta$ . Thus, in the thermodynamic limit  $\hat{U}_1 = I + O(\frac{1}{L})$  on the left (right) Wannier functions and hence  $\det(\mathcal{L}) = 1 + O(\frac{1}{L})$  [ $\det(\mathcal{R}) = 1 + O(\frac{1}{L})$ ]. Therefore,

$$\lim_{L \rightarrow \infty} \frac{1}{2\pi} \text{Im}[\log(\langle U_1 \rangle)] = \sum_{\alpha=1}^{N_{\text{occ}}} \nu_{\alpha} = Q_c^{(1)}, \quad (\text{C4})$$

where the last equality follows from the original bulk-boundary correspondence [17,23]. This completes the proof that the  $\hat{U}_1$  expectation value reproduces the boundary charge for band insulators in the open boundary condition.

#### APPENDIX D: COORDINATE DEPENDENCE OF $\phi_{op}$

In this Appendix, we discuss the coordinate dependence of the phase factors  $\{\phi_{op}\}$  defined in Eq. (13). The phase factor  $\phi_{op}$  is computed on a system having periodic boundary conditions along the  $y$  direction, i.e., the system is invariant under the coordinate transformation along that direction  $y \rightarrow y + L_y$ . Thus, one naturally expects that the phase factors should also be invariant under the coordinate transformation. Here, we show that if the system size is sufficiently large, then the phase factors are invariant under the coordinate transformation.

We first treat the system as a quasi-1D system by considering the  $y$  label as a sublattice index of the enlarged unit cell. We then consider the transformation rule for the  $\hat{U}_2$  operator:  $\hat{U}_2 \rightarrow \hat{U}'_2 = \hat{U}_2 \hat{U}_{1,x}$  following from the translation along the periodic direction  $y \rightarrow y + L_y$ , where  $\hat{U}_{1,x}$  is

$$\hat{U}_{1,x} = \exp \left[ \frac{2\pi i}{L_x} \sum_{x,y=1}^{L_x, L_y} x(\hat{n}_{x,y} - n_e) \right] \quad (\text{D1})$$

with the background charge  $n_e$ . Since we consider the system as a quasi-1D system, the additional operator  $\hat{U}_{1,x}$  can be viewed as Resta's  $\hat{U}_1$  operator Eq. (3). Although  $|\text{GS}(o, p)\rangle$  is not an eigenstate of  $\hat{U}_{1,x}$  in general, it converges to an eigenstate of  $\hat{U}_{1,x}$  in the limit of  $L_x \rightarrow \infty$ . We can show this in the following two steps. First, if the system size is sufficiently large, then the expectation value of  $\hat{U}_{1,x}$  with  $|\text{GS}(o, p)\rangle$  is bounded by

$$|1 - \langle \text{GS}(o, p) | \hat{U}_{1,x} | \text{GS}(o, p) \rangle| \leq \mathcal{C} \frac{L_y}{L_x} \quad (\text{D2})$$

with some constant  $\mathcal{C}$ . This can be seen from Eq. (C3). Second, since  $\hat{U}_{1,x}$  is a unitary operator, the absolute value of its expectation value with a state is unity if and only if the state is an eigenstate of  $\hat{U}_{1,x}$ . Thus, Eq. (D2) implies that  $|\text{GS}(o, p)\rangle$  is an eigenstate of  $\hat{U}_{1,x}$  in the limit of  $L_x \rightarrow \infty$ . With these, the expectation value of  $\hat{U}'_2$  with  $|\text{GS}(o, p)\rangle$  can be written as that of  $\hat{U}_2$  in the limit of  $L_x \rightarrow \infty$ :

$$\begin{aligned} e^{i\tilde{\phi}_{op}} &\equiv \langle \text{GS}(o, p) | \hat{U}'_2 | \text{GS}(o, p) \rangle \\ &= e^{i\phi_{op}} \langle \text{GS}(o, p) | \hat{U}_{1,x} | \text{GS}(o, p) \rangle. \end{aligned} \quad (\text{D3})$$

Thus, the only thing we need to show is that the additional term  $\langle \text{GS}(o, p) | \hat{U}_{1,x} | \text{GS}(o, p) \rangle$  converges to unity in the thermodynamic limit.

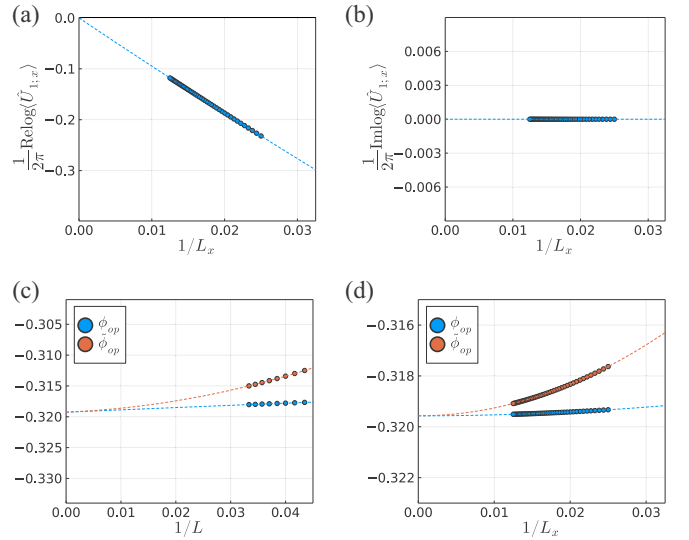


FIG. 4. (a-b) Fittings of (a) real and (b) imaginary parts of  $\langle \hat{U}_{1,x} \rangle = \langle \text{GS}(o, p) | \hat{U}_{1,x} | \text{GS}(o, p) \rangle$  on  $H_{\text{edge}}$  with  $L_x > L_y = 10$  using quadratic polynomials in  $1/L_x$ .  $\langle \hat{U}_{1,x} \rangle$  converges to unity in the limit of  $L_x \rightarrow \infty$ . (c-d) Fittings of the phase factors  $\phi_{op}$  and  $\tilde{\phi}_{op}$  on  $H_{\text{edge}}$  in (c) isotropic systems,  $L_x = L_y = L$ , and (d) anisotropic systems  $L_x > L_y = 10$  using quadratic polynomials in  $1/L$  and  $1/L_x$ , respectively. Both of them converge to the same value in the limit of (c)  $L \rightarrow \infty$  and (d)  $L_x \rightarrow \infty$ .

Now, we will show that  $\langle \text{GS}(o, p) | \hat{U}_{1,x} | \text{GS}(o, p) \rangle$  indeed converges to unity in the thermodynamic limit. Since we treat the system as a quasi-1D system,  $\langle \text{GS}(o, p) | \hat{U}_{1,x} | \text{GS}(o, p) \rangle$  can be interpreted as  $e^{i\phi_o}$  defined in Eq. (6). In Appendix C, we show that  $\phi_o$  can be identified with the boundary charge in the limit of  $L_x \rightarrow \infty$ . In addition, since the polarization of each model is vanishing to make the quadrupole moment be well defined, the quasi-1D system cannot have the polarization as well as the boundary charge. Combining these implies that  $\langle \text{GS}(o, p) | \hat{U}_{1,x} | \text{GS}(o, p) \rangle$  should converge to unity in the thermodynamic limit, and thus  $e^{i\phi_{op}}$  in the thermodynamic limit is invariant under  $y \rightarrow y + L_y$ .

As an explicit demonstration of our proof above, we first conduct numerical calculations on  $\langle \text{GS}(o, p) | \hat{U}_{1,x} | \text{GS}(o, p) \rangle$  and find that it converges to unity in the thermodynamic limit. Here, we consider the edge-localized polarization insulator, which is defined in Eq. (21). We choose the parameters as  $(\gamma_x, \gamma_y, \lambda_x, \lambda_y, \delta) = (0.2, 0.3, 1.0, 1.0, 0.1)$ . We then compute real and imaginary parts of  $\log[\langle \text{GS}(o, p) | \hat{U}_{1,x} | \text{GS}(o, p) \rangle]$  on anisotropic systems  $L_x \neq L_y$  with  $L_y = 10$  and  $L_x$  from 40 to 80. We extrapolate them in the thermodynamic limit as a function of  $1/L_x$ . The extrapolations of them are shown in Figs. 4(a) and 4(b) which are for real and imaginary parts, respectively. These clearly show that  $\langle \text{GS}(o, p) | \hat{U}_{1,x} | \text{GS}(o, p) \rangle$  converges to unity in the thermodynamic limit.

The above argument only guarantees the invariance of  $\phi_{op}$  under the transformation  $y \rightarrow y + L_y$  when we take the limit of  $L_x \rightarrow \infty$  first since the right-hand side of Eq. (D2) may not converge for other orders of limits. However, even for those cases, we numerically check that  $\phi_{op}$  is still invariant under the coordinate transformation. Below, we provide numerical calculations on  $\phi_{op}$ , and for those cases, one can see that the

phase factor is invariant under the transformation  $y \rightarrow y + L_y$  in the thermodynamic limit.

We compute the phase factor  $\phi_{op}$  and the transformed phase factor  $\tilde{\phi}_{op}$  [Eq. (D3)] on the same system used in this section. However, here, we separately compute them on (1) isotropic systems  $L_x = L_y = L$  with  $L$  from 23 to 30 and (2) anisotropic systems  $L_x \neq L_y$  with  $L_y = 10$  and  $L_x$  from 40 to 80. We then extrapolate  $\phi_{op}$  and  $\tilde{\phi}_{op}$  in the thermodynamic limit via quadratic extrapolations as a function of  $1/L_x$ . The extrapolations of  $\phi_{op}$  and  $\tilde{\phi}_{op}$  on the edge-localized polarization insulator are shown in Figs. 4(c) and 4(d), which are for (1) isotropic systems and (2) anisotropic systems, respectively. The numerical results clearly show that the transformation  $y \rightarrow y + L_y$  does not change the thermodynamic value of  $\phi_{op}$ .

In addition, we also compute  $\phi_{op}$  and  $\tilde{\phi}_{op}$  when the limit of  $L_y \rightarrow \infty$  is taken first. We first extrapolate  $\phi_{op}$  and  $\tilde{\phi}_{op}$  as quadratic functions of  $L_y$  for various  $L_x \in [10, 20]$  as shown in Fig. 5. From this, we get the thermodynamic values of  $\phi_{op}$  and  $\tilde{\phi}_{op}$  in the quasi-1D system  $L_y \rightarrow \infty$ . We then extrapolate those thermodynamic values as quadratic functions of  $L_x$  as shown in Fig. 5. One can see from Fig. 5 that the extrapolated values of  $\phi_{op}$  and  $\tilde{\phi}_{op}$  in the quasi-1D system agree with that of  $\phi_{op}$  in the 2D system  $L_x = L_y = L \rightarrow \infty$ . Thus, even we take the limit of  $L_y \rightarrow \infty$  first,  $\phi_{op}$  and  $\tilde{\phi}_{op}$  agree in the thermodynamic limit on this case.

### APPENDIX E: SUM RULE IN THE $C_3$ -SYMMETRIC INSULATOR

As a demonstration that the sum rule Eq. (14) works for insulators having other types of symmetry besides  $C_4$  symmetry, we consider a  $C_3$ -symmetric insulator [24] and numerically confirm the sum rule on this model.

#### 1. $C_3$ -symmetric insulator: $H_{2b}^{(3)} \oplus H_{2c}^{(3)}$

The tight-binding Hamiltonian in the momentum space of the  $C_3$ -symmetric insulator  $H_{2b}^{(3)} \oplus H_{2c}^{(3)}$  is given by [24]

$$H_{2b}^{(3)} \oplus H_{2c}^{(3)}(\mathbf{k}) = \begin{bmatrix} H_{2b}^{(3)} & \gamma^{(3)}(t) \\ \gamma^{(3)}(t)^\dagger & H_{2c}^{(3)} \end{bmatrix}, \quad (\text{E1})$$

where

$$H_{2b}^{(3)}(\mathbf{k}) = \begin{bmatrix} 0 & t_0 + e^{ik \cdot \mathbf{a}_2} & t_0 + e^{-ik \cdot \mathbf{a}_3} \\ t_0 + e^{-ik \cdot \mathbf{a}_2} & 0 & t_0 + e^{-ik \cdot \mathbf{a}_1} \\ t_0 + e^{ik \cdot \mathbf{a}_3} & t_0 + e^{ik \cdot \mathbf{a}_1} & 0 \end{bmatrix},$$

$$H_{2c}^{(3)}(\mathbf{k}) = \begin{bmatrix} 0 & t_0 + e^{ik \cdot \mathbf{a}_1} & t_0 + e^{ik \cdot \mathbf{a}_2} \\ t_0 + e^{-ik \cdot \mathbf{a}_1} & 0 & t_0 + e^{-ik \cdot \mathbf{a}_3} \\ t_0 + e^{-ik \cdot \mathbf{a}_2} & t_0 + e^{ik \cdot \mathbf{a}_3} & 0 \end{bmatrix},$$

and

$$\gamma^{(3)}(t) = \begin{bmatrix} t & t & 0 \\ 0 & t & t \\ t & t & 0 \end{bmatrix}. \quad (\text{E2})$$

The  $2/3$ -filled ground states of  $H_{2b}^{(3)}$  and  $H_{2c}^{(3)}$  have nonvanishing polarizations  $1/3$  and  $2/3$ , respectively, so the stacked model  $H_{2b}^{(3)} \oplus H_{2c}^{(3)}$  at  $2/3$  filling with the interlayer hopping term  $\gamma^{(3)}(t)$  has vanishing bulk polarization and respects  $C_3$  symmetry.

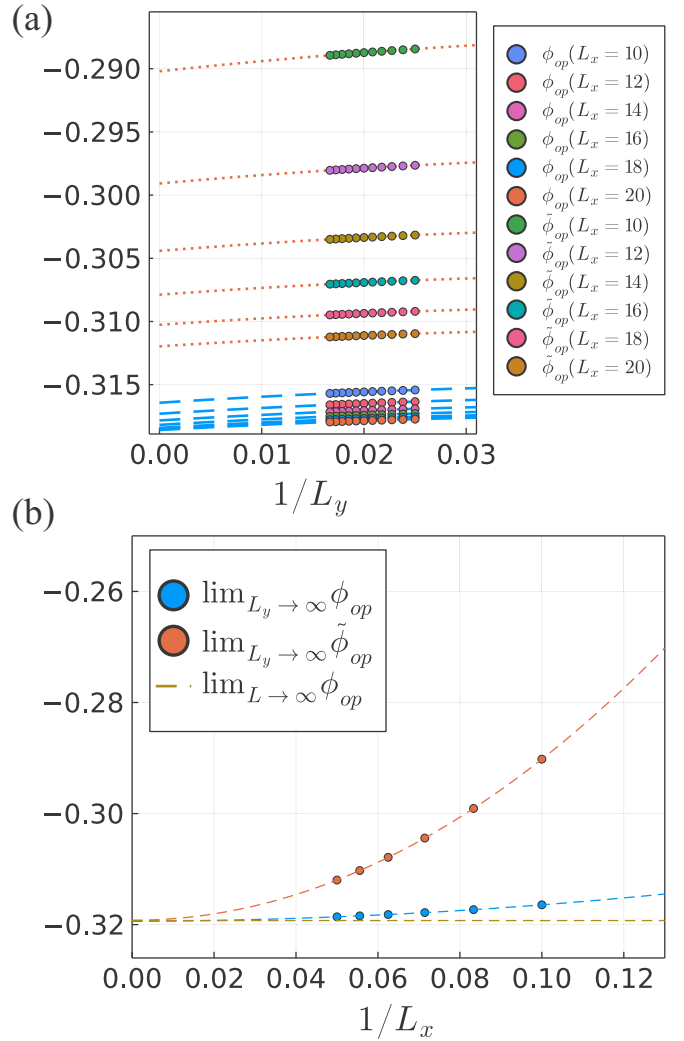


FIG. 5. (a) Fittings of  $\phi_{op}$  and  $\tilde{\phi}_{op}$  using quadratic polynomials in  $1/L_y$  while fixing  $L_x$ . The blue dashed lines are quadratic extrapolations of  $\phi_{op}$  and the orange dotted lines are quadratic extrapolations of  $\tilde{\phi}_{op}$ . (b) Fittings of  $\lim_{L_y \rightarrow \infty} \phi_{op}$  and  $\lim_{L_y \rightarrow \infty} \tilde{\phi}_{op}$  using quadratic polynomials in  $1/L_x$ . The ochre dashed line is the thermodynamic value of  $\phi_{op}$  in the 2D system. Each y-intercept of an extrapolation in (a) is a point in (b).

We will consider the stacked model Eq. (E1) on the square lattice. To do so, we use the coordinates system  $(x, y)$  with two basis vectors  $\vec{a}_1 = (1, 0)$  and  $\vec{a}_2 = (1/2, \sqrt{3}/2)$ , i.e., the coordinates  $(x, y)$  refer to as the vector of  $x\vec{a}_1 + y\vec{a}_2$ . All the phase factors  $\phi_{ab}$  defined in Eq. (13) and appearing in Table VII are computed using these coordinates. We find that the stacked model on the square lattice at  $2/3$  filling has corner charges  $1/3$  and  $-1/3$  well localized near the corners.

The numerical results are summarized in Table VII. We see that the corner charge  $Q_c^{(2)}$  agrees with  $\phi_{oo}$  and the sum rule Eq. (14) is satisfied up to small errors of  $O(10^{-5})$ .

### APPENDIX F: BRANCH CUT DEPENDENCE OF THE HWF-BASED EDGE-LOCALIZED POLARIZATION

In this section, we discuss the branch cut dependence in the hybrid Wannier values of the HWF-based edge-localized

TABLE VII. The phase factors  $\phi_{ab}$  and the corner charge  $Q_c^{(2)}$  are computed for  $H_{2b}^{(3)} \oplus H_{2c}^{(3)}(t_0, t)$  in Eq. (E1) on a square lattice with various parameters. The details about the lattice and filling are discussed in the paragraph below Eq. (E2). Here we use the same extrapolation procedure as in Table I. The corner charge agrees with  $\phi_{oo}$  and the sum rule Eq. (14) is satisfied up to small errors.

Model parameters $H_{2b}^{(3)} \oplus H_{2c}^{(3)}(t_0, t)$	Phase factors				Electric moment	Sum rule
	$\phi_{pp}$	$\phi_{po}$	$\phi_{op}$	$\phi_{oo}$	$Q_c^{(2)}$	$\sum (-1)^{ab} \phi_{ab}$
(0.001,0.001)	-0.33340(0)	-0.33333(0)	-0.33333(0)	-0.33331(0)	-0.33333(0)	-0.00005(0)
(0.1,0.001)	-0.33340(0)	-0.33335(0)	-0.33335(0)	-0.33334(0)	-0.33337(0)	-0.00005(0)
(0.1,0.1)	-0.33377(0)	-0.33441(0)	-0.33441(0)	-0.33510(0)	-0.33513(0)	-0.00004(0)
(0.2,0.1)	-0.33380(0)	-0.33504(0)	-0.33504(0)	-0.33631(0)	-0.33634(0)	-0.00004(0)

polarization  $\tilde{P}_{x/y}^{\text{edge}}$  defined in Ref. [4] and Eq. (18). To be self-contained, we first rewrite the definition of the edge-localized polarization:

$$\tilde{P}_x^{\text{edge}} = \sum_j \sum_{y=1}^{L_y/2} v^j \rho^j(y) \pmod{1}, \quad (\text{F1})$$

where  $\rho^j(y)$  and  $e^{2\pi i v_j}$  are the density and the  $j$ th eigenvalue of the hybrid Wilson loop  $\mathcal{W}_{k_x}$  along the  $x$  direction, respectively. We will call  $v^j$  the hybrid Wannier value.

The edge-localized polarization  $\tilde{P}_x^{\text{edge}}$  can be well defined after one fixes the branch cut of the hybrid Wannier value since the hybrid Wannier value is defined by a phase angle, which has the modulo  $2\pi$  ambiguity. Unless fixing the branch cut, each  $v^j$  can be shifted by an integer  $n^j = \pm 1$ , which results in shifting  $\tilde{P}_x^{\text{edge}}$  as

$$\Delta \tilde{P}_x^{\text{edge}} = \sum_j \sum_{y=1}^{L_y/2} n^j \rho^j(y). \quad (\text{F2})$$

Since  $\sum_{y=1}^{L_y/2} \rho^j(y)$  is not quantized in general,  $\Delta \tilde{P}_x^{\text{edge}}$  may also not be quantized if  $n^j$  is not the same for all  $j$ .

Consequently, the edge-localized polarization is ambiguous before fixing the branch cut even if we take the modulo one equivalence on both sides of Eq. (F1). Here we fix the branch cut by fixing the range of the hybrid Wannier value as  $v \in (-0.5, 0.5]$ . This choice is made for our numerical results to be consistent with that of Ref. [4]. Note that another equally valid choice of the range is  $v \in [-0.5, 0.5)$ , which includes  $-0.5$  instead of  $+0.5$ .

However, these possibilities in ranges again cause a problem when a hybrid Wannier value  $v^j$  is at the branch cut value since  $v^j$  can be either  $+0.5$  or  $-0.5$  depending on the choice of the range. In this case, the edge-localized polarization is invariant under the choice of the range only when  $\sum_{y=1}^{L_y/2} \rho^j(y)$  is quantized, i.e., the HWF is localized in one of the two half systems. The situation gets worse when more than two hybrid Wannier values  $v^1, v^2, \dots, v^n$  are degenerated at the branch cut since, for all possible unitary transformations  $\tilde{\psi}^i(y) = \sum_{j=1}^n u_{ij} \psi^j(y)$  of the Wannier functions  $\{\psi^1, \psi^2, \dots, \psi^n\}$ ,  $\sum_{y=1}^{L_y/2} |\tilde{\psi}^i(y)|^2$  should be quantized for the edge-localized polarization not to depend sensitively on the choice of the branch cut. To avoid this difficulty, we computed  $\tilde{P}_{x/y}^{\text{edge}}$  only for the models without the hybrid Wannier value at 0.5 in the main text.

- [1] M. Z. Hasan and C. L. Kane, Colloquium: Topological insulators, *Rev. Mod. Phys.* **82**, 3045 (2010).
- [2] X.-L. Qi and S.-C. Zhang, Topological insulators and superconductors, *Rev. Mod. Phys.* **83**, 1057 (2011).
- [3] W. A. Benalcazar, B. A. Bernevig, and T. L. Hughes, Quantized electric multipole insulators, *Science* **357**, 61 (2017).
- [4] W. A. Benalcazar, B. A. Bernevig, and T. L. Hughes, Electric multipole moments, topological multipole moment pumping, and chiral hinge states in crystalline insulators, *Phys. Rev. B* **96**, 245115 (2017).
- [5] F. Schindler, A. M. Cook, M. G. Vergniory, Z. Wang, S. S. P. Parkin, B. A. Bernevig, and T. Neupert, Higher-order topological insulators, *Sci. Adv.* **4**, eaat0346 (2018).
- [6] M. J. Park, Y. Kim, G. Y. Cho, and S. Lee, Higher-Order Topological Insulator in Twisted Bilayer Graphene, *Phys. Rev. Lett.* **123**, 216803 (2019).
- [7] H. Watanabe and H. C. Po, Fractional Corner Charge of Sodium Chloride, *Phys. Rev. X* **11**, 041064 (2021).
- [8] Y. Liu, S. Leung, F.-F. Li, Z.-K. Lin, X. Tao, Y. Poo, and J.-H. Jiang, Bulk-disclination correspondence in topological crystalline insulators, *Nature (London)* **589**, 381 (2021).
- [9] C. W. Peterson, T. Li, W. A. Benalcazar, T. L. Hughes, and G. Bahl, A fractional corner anomaly reveals higher-order topology, *Science* **368**, 1114 (2020).
- [10] L. Fu and C. L. Kane, Time reversal polarization and a  $Z_2$  adiabatic spin pump, *Phys. Rev. B* **74**, 195312 (2006).
- [11] S. Coh and D. Vanderbilt, Electric Polarization in a Chern Insulator, *Phys. Rev. Lett.* **102**, 107603 (2009).
- [12] T. L. Hughes, E. Prodan, and B. A. Bernevig, Inversion-symmetric topological insulators, *Phys. Rev. B* **83**, 245132 (2011).
- [13] R. Yu, X. L. Qi, A. Bernevig, Z. Fang, and X. Dai, Equivalent expression of  $Z_2$  topological invariant for band insulators using the non-Abelian Berry connection, *Phys. Rev. B* **84**, 075119 (2011).
- [14] A. Alexandradinata, X. Dai, and B. A. Bernevig, Wilson-loop characterization of inversion-symmetric topological insulators, *Phys. Rev. B* **89**, 155114 (2014).
- [15] R. D. King-Smith and D. Vanderbilt, Theory of polarization of crystalline solids, *Phys. Rev. B* **47**, 1651 (1993).
- [16] R. Resta, Macroscopic electric polarization as a geometric quantum phase, *Europhys. Lett.* **22**, 133 (1993).

- [17] D. Vanderbilt and R. D. King-Smith, Electric polarization as a bulk quantity and its relation to surface charge, *Phys. Rev. B* **48**, 4442 (1993).
- [18] R. Resta, Quantum-Mechanical Position Operator in Extended Systems, *Phys. Rev. Lett.* **80**, 1800 (1998).
- [19] H. Watanabe and S. Ono, Corner charge and bulk multipole moment in periodic systems, *Phys. Rev. B* **102**, 165120 (2020).
- [20] B. Kang, K. Shiozaki, and G. Y. Cho, Many-body order parameters for multipoles in solids, *Phys. Rev. B* **100**, 245134 (2019).
- [21] W. A. Wheeler, L. K. Wagner, and T. L. Hughes, Many-body electric multipole operators in extended systems, *Phys. Rev. B* **100**, 245135 (2019).
- [22] S. Ono, L. Trifunovic, and H. Watanabe, Difficulties in operator-based formulation of the bulk quadrupole moment, *Phys. Rev. B* **100**, 245133 (2019).
- [23] J.-W. Rhim, J. Behrends, and J. H. Bardarson, Bulk-boundary correspondence from the intercellular Zak phase, *Phys. Rev. B* **95**, 035421 (2017).
- [24] W. A. Benalcazar, T. Li, and T. L. Hughes, Quantization of fractional corner charge in  $C_n$ -symmetric higher-order topological crystalline insulators, *Phys. Rev. B* **99**, 245151 (2019).
- [25] R. Takahashi, T. Zhang, and S. Murakami, General corner charge formula in two-dimensional  $C_n$ -symmetric higher-order topological insulators, *Phys. Rev. B* **103**, 205123 (2021).
- [26] Y. Fang and J. Cano, Filling anomaly for general two- and three-dimensional  $C_4$  symmetric lattices, *Phys. Rev. B* **103**, 165109 (2021).
- [27] M. Jung, Y. Yu, and G. Shvets, Exact higher-order bulk-boundary correspondence of corner-localized states, *Phys. Rev. B* **104**, 195437 (2021).
- [28] S. Kooi, G. van Miert, and C. Ortix, The bulk-corner correspondence of time-reversal symmetric insulators, *npj Quantum Mater.* **6**, 1 (2021).
- [29] L. Trifunovic, Bulk-and-edge to corner correspondence, *Phys. Rev. Research* **2**, 043012 (2020).
- [30] S. Ren, I. Souza, and D. Vanderbilt, Quadrupole moments, edge polarizations, and corner charges in the Wannier representation, *Phys. Rev. B* **103**, 035147 (2021).
- [31] X. Ying, Change of corner charge and adiabatic current distribution in two dimensional insulators with inversion symmetry, [arXiv:2109.10395](https://arxiv.org/abs/2109.10395).
- [32] L. Trifunovic, S. Ono, and H. Watanabe, Geometric orbital magnetization in adiabatic processes, *Phys. Rev. B* **100**, 054408 (2019).
- [33] Y. Zhou, K. M. Rabe, and D. Vanderbilt, Surface polarization and edge charges, *Phys. Rev. B* **92**, 041102(R) (2015).
- [34] A. Daido, A. Shitade, and Y. Yanase, Thermodynamic approach to electric quadrupole moments, *Phys. Rev. B* **102**, 235149 (2020).
- [35] H. Shapourian, K. Shiozaki, and S. Ryu, Many-Body Topological Invariants for Fermionic Symmetry-Protected Topological Phases, *Phys. Rev. Lett.* **118**, 216402 (2017).
- [36] G. Y. Cho, C.-T. Hsieh, T. Morimoto, and S. Ryu, Topological phases protected by reflection symmetry and cross-cap states, *Phys. Rev. B* **91**, 195142 (2015).
- [37] K. Shiozaki, H. Shapourian, K. Gomi, and S. Ryu, Many-body topological invariants for fermionic short-range entangled topological phases protected by antiunitary symmetries, *Phys. Rev. B* **98**, 035151 (2018).
- [38] B. Kang, W. Lee, and G. Y. Cho, Many-Body Invariants for Chern and Chiral Hinge Insulators, *Phys. Rev. Lett.* **126**, 016402 (2021).
- [39] Z.-P. Cian, H. Dehghani, A. Elben, B. Vermersch, G. Zhu, M. Barkeshli, P. Zoller, and M. Hafezi, Many-Body Chern Number from Statistical Correlations of Randomized Measurements, *Phys. Rev. Lett.* **126**, 050501 (2021).
- [40] S. Kivelson, Wannier functions in one-dimensional disordered systems: Application to fractionally charged solitons, *Phys. Rev. B* **26**, 4269 (1982).